LATE CENOZOIC FAULTS OF THE REGION SURROUNDING THE EAGLE FLAT STUDY AREA, NORTHWESTERN TRANS-PECOS TEXAS

by

Edward W. Collins and Jay A. Raney

Final Report

Prepared for

Texas Low-Level Radioactive Waste Disposal Authority
under Interagency Contract Number IAC(92-93)-0910

Bureau of Economic Geology
W. L. Fisher, Director
The University of Texas at Austin
Austin, Texas 78713-7508

September 1993

CONTENTS

Figures

Tables

EXECUTIVE SUMMARY

The Eagle Flat study area is located along the southeastern edge of the southern Basin and Range–Rio Grande tectonic province in Trans-Pecos Texas. The desert region that encompasses the study area consists of the broad Diablo Plateau and a series of mountain ranges and adjacent intermontane basins that formed by extensional faulting that probably occurred in the last 24 mya. There has been no historical surface rupturing of faults in Trans-Pecos Texas, although earthquakes have occurred and faults that displace Quaternary (present to approximately 2 mya) deposits are present (fig. 1). Geologic investigations of faults active during the Quaternary provide important data (tables A-1 and A-2) for seismic risk studies of the proposed Eagle Flat low-level radioactive waste repository.

Most of the Quaternary faults of Trans-Pecos Texas are between about 11 and 24.8 mi (18 and 40 km) long (table A-1). Many of the faults are sections of longer fault zones that are between 43 and 64 mi (70 and 105 km) long. Strikes of individual faults are variable, although most of the fault zones strike northwestward or northward. Faults dip between 50° and 89°. Fourteen Quaternary faults are within 31 mi (50 km) of the proposed repository.

The northwest Eagle Flat Basin, the location of the proposed repository, is a relatively shallow basin with a maximum basin-fill thickness of <900 ft (<270 m). Most of the basin contains less than 500 ft (150 m) of sediments. The relatively shallow thickness of the basin-fill deposits in the northwest Eagle Flat Basin suggests that the faults that formed this basin were not as active as faults that formed the deeper intermontane basins such as the Hueco Bolson that contains as much as 8,800 to 9,800 ft (2,700 to 3,000 m) of basin-fill deposits. Within the northwest Eagle Flat Basin, there are no fault scarps cutting young (present to about 500,000 yr) surficial sediments. Surface bedrock geology and subsurface data from drill holes and seismic reflection data suggest that several subsurface faults may cut Cretaceous and older rocks underlying the Cenozoic basin-fill sediments. It is possible that some of the faults were active

during the earlier development (Pliocene or Miocene, 2.5 to 24 mya) of northwest Eagle Flat Basin.

The closest Quaternary fault scarp to the proposed repository is 8.4 mi (13.5 km) south in the Red Light Bolson. This dissected, 4.3-mi-long (7-km) scarp is part of the West Eagle Mountains–Red Hills fault that bounds the east margin of the northern Red Light Bolson. Analysis of possible earthquake magnitudes and ground accelerations related to this fault may set the earthquake design parameters for the proposed repository. The West Eagle Mountains–Red Hills fault is as long as 24.8 mi (40 km), on the basis of assuming that much of the fault's surface expression has been eroded or is covered along the western margin of Devils Ridge and most of the western edge of the Eagle Mountains. The closest distance from the proposed repository to an inferred part of this fault is 6.5 mi (10.5 km). The fault strikes N25°–55°W and dips southwestward. The scarp is 4.6 to 13 ft (1.4 to 4 m) high and cuts middle Pleistocene alluvial-fan deposits that are capped by an approximately 3-ft-thick (1-m) stage IV pedogenic calcrete on the upthrown fault block. The scarp is dissected and subtle, and the scarp-slope angle is locally only as much as 4°. A 11.5-ft-deep (3.5-m) trench that was excavated across the fault trace revealed that the fault dips 85° to 88° southwest and cuts gravelly deposits that include two faulted buried calcic soils on the downthrown block as well as a near-surface faulted calcic soil. There have been three surface ruptures since the middle Pleistocene. Throws for the surface-rupture events were between 1.6 and 4.2 ft (0.5 and 1.3 m). Maximum cumulative throw on middle Pleistocene deposits (fig. 3), which are approximately 250,000 to 500,000 yr old on the basis of the calcic soil development, is 9 ft (2.7 m). Throw on middle-upper Pleistocene deposits (fig. 3), which are approximately 25,000 to 250,000 yr old on the basis of the calcic soil development, is 1.6 ft (0.5 m). In the trench, fractures are not visible across the fault in the upper 8 to 12 inches (20 to 30 cm) of the calcic horizon at the surface. We postulate that postfaulting soil forming processes have obscured the upper part of the fault. The approximate average slip rate of the West Eagle Mountains–Red Hills fault since the middle

Pleistocene is ≤0.02 mm/yr. The average recurrence interval for large surface ruptures since the middle Pleistocene is about 80,000 to 160,000 yr, assuming three surface paleoruptures.

The average slip rates since middle Pleistocene for Quaternary faults in Trans-Pecos Texas are relatively low at <0.25 mm/yr (table A-2). Most of the Quaternary faults have average slip rates of ≤0.1 mm/yr. The maximum amount of throw during surface paleoruptures was between 1.6 and 10 ft (0.5 and 3 m). Throw of middle Pleistocene deposits (fig. 3) having stage IV pedogenic calcrete ranges between 3 and 105 ft (1 and 32 m). At least eight faults cut upper Pleistocene deposits (fig. 3), and throws are between 3 and 20 ft (1 and 6 m). Aerial-photograph studies of faulted areas not investigated on the ground suggest that several other faults probably displace upper Pleistocene (fig. 3) or younger deposits. Average recurrence intervals since the middle Pleistocene (fig. 3) for most of the faults are approximately 50,000 to 160,000 yr.

The most active faults of the region include the East Franklin Mountains fault that is 86 mi (138 km) west of the proposed repository and the fault sections of the Amargosa fault zone that are between 25 and 38 mi (41 and 62 km) from the proposed repository. These faults have scarps in probable Holocene deposits and vertically displace upper Pleistocene deposits (fig. 3) as much as 15 to 20 ft (4.5 to 6 m), suggesting multiple upper Pleistocene–Holocene (fig. 3) ruptures. The closest fault to the proposed repository that may have ruptured during the late Pleistocene–Holocene (fig. 3) is the West Indio Mountains fault, which is 21.4 mi (34.5 km) south of the proposed site.

INTRODUCTION

The Eagle Flat study area is located along the southeastern edge of the southern Basin and Range–Rio Grande Rift tectonic province in Trans-Pecos Texas (fig. 1). Geologic features of the region record a long history of geologic events (Henry and Price, 1985; Muehlberger and Dickerson, 1989; Raney and Collins, 1993). This report discusses late Cenozoic faults of the region that have ruptured during the Quaternary. During the Cenozoic Era, intermontane

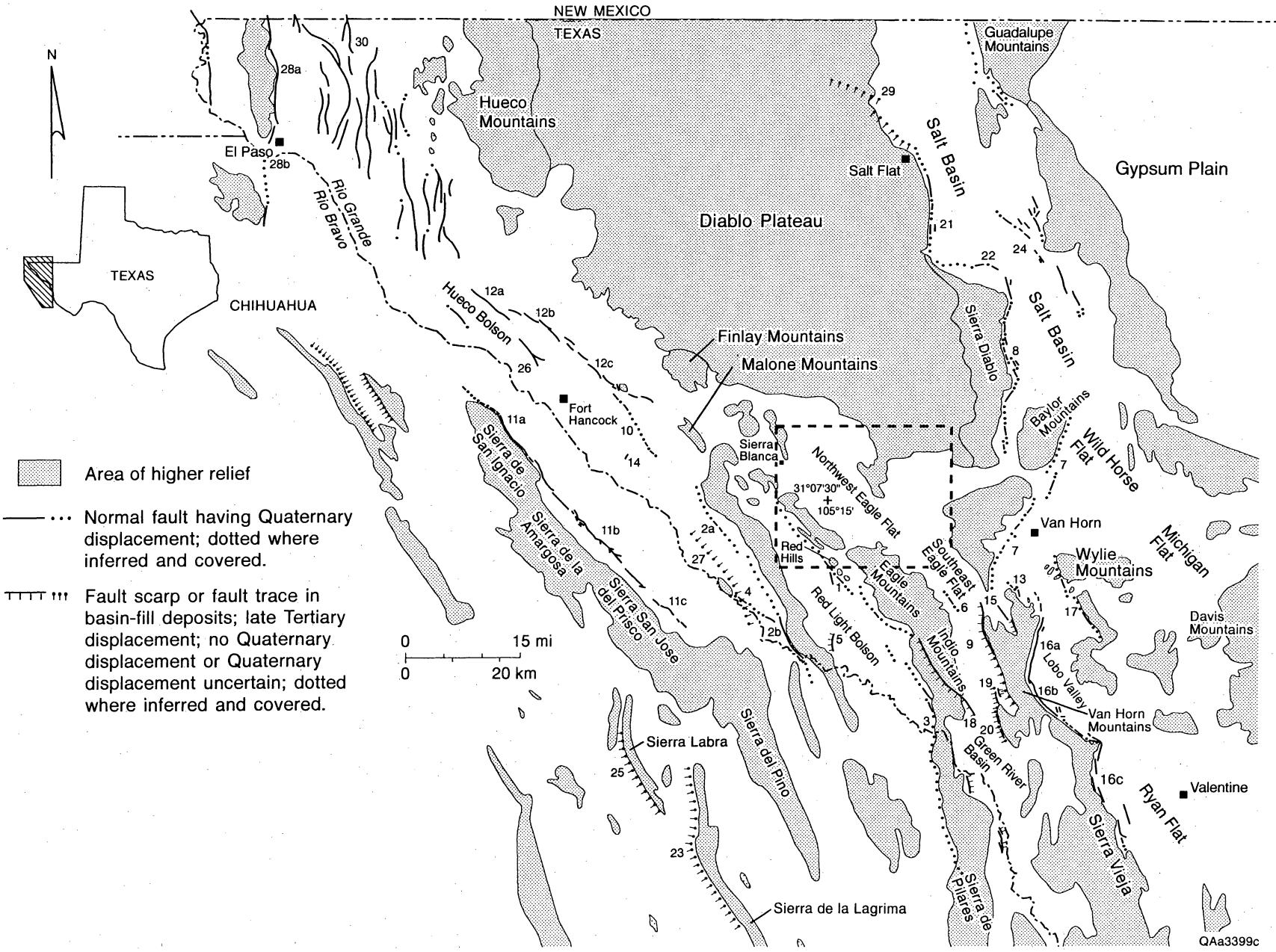

Figure 1. Regional map of Quaternary faults, northwestern Trans-Pecos Texas. Numbers identify faults discussed in text. Dashed rectangle indicates the Eagle Flat study area. The latitude 31°07'30", longitude 105°15' reference point is near the proposed repository site on Faskin Ranch.

basins and associated normal faults formed in response to Basin and Range extensional tectonism that began about 24 mya (Henry and Price, 1985, 1986). There has been no historical surface rupturing of faults in West Texas, although earthquakes have occurred and faults that displace Quaternary (present to approximately 2 mya) deposits are present.

Geologic investigations of faults active during the Quaternary provide important data for seismic risk studies of the proposed Eagle Flat low-level radioactive waste repository. Fault characteristics described for this investigation include fault lengths, strikes, dips, and dip directions, distances between faults and the proposed repository, amounts of slip on Quaternary deposits, amounts of throw for paleoseismic surface rupture events, average slip rates, and average recurrence intervals between large paleoruptures.

Location and Methods

The study area includes a region of Trans-Pecos Texas, and Chihuahua, Mexico, that is more than 50 km (>31 mi) from the proposed repository site, which is located on the Faskin Ranch within the northwest Eagle Flat area (fig. 1). Our results were derived from aerial photograph and field geologic mapping, field observations, and measurements of fault scarps, outcrops, and excavations. Aerial photographs were studied to identify fault scarps, to aid in mapping faults and faulted deposits, and to identify specific areas along the faults for detailed field studies. Aerial photographs used in this study were: (1) 1991 black-and-white photographs, 1:6,000 scale; (2) 1980 color photographs, 1:24,000 scale; (3) 1972 black-and-white photographs, scales 1:32,000 and 1:26,000; (4) 1963 black-and-white photographs, scale 1:28,000; (5) 1957 black-and-white photographs, scale 1:62,000; and (6) 1948 black-and-white photographs, scale 1:43,000. We flew over parts of the area at low altitudes in a fixed-wing aircraft to review aerial-photograph interpretations. Seismic reflection data also were interpreted for some parts of the region to provide subsurface information on faults.

The base maps we used included U.S. Geological Survey 7.5-minute quadrangle maps (scale 1:24,000), several Secretaria de Programacion y Presupuesto topographic maps of Chihuahua, Mexico, including the Guadalupe D. B., Esperanza, Las Palmas, Porvenir, El Consuelo, Banderas, and Cajoncitos sheets (scale 1:50,000), and the U.S. Geological Survey Van Horn–El Paso and Marfa 2-degree topographic maps (scale 1:250,000), the Van Horn, Marfa, and El Paso Joint Operations Graphic (ground) maps (scale 1:250,000). Distances of faults to a reference point on the Faskin Ranch within northwest Eagle Flat, latitude 105°15' and longitude 31°07'30", are reported. Scarp heights, measured using an Abney level, usually do not reflect the exact amount of vertical offset across faulted geomorphic surfaces because the geomorphic surfaces are sloping, the scarps are eroded, and colluvial deposits often are deposited on faulted downthrown surfaces. Scarp heights and slopes are reported; however, quantitative analyses to estimate the ages of scarps (Wallace, 1977; Bucknam and Anderson, 1979) were not done because the variations in the geomorphic settings and physical properties (grain size, cementation, composition, etc.) of the faulted deposits at different scarps, combined with the different amounts of data we collected at the different scarps, prevented an accurate comparison of the scarps.

Precise ages of faulted Quaternary (present to approximately 2 mya) and Tertiary (approximately 2 to 66.4 mya) deposits have not been determined because these deposits have few materials suitable for accurate dating. Relative ages have been estimated on the basis of field stratigraphic relationships, the degree of calcic soil development (Gile and others, 1966, 1981; Machette, 1985), and correlation with similar units in south-central New Mexico (Hawley, 1975; Gile and others, 1981).

Our estimates of fault slip rates and the ranges of the average recurrence interval for large surface ruptures since the middle Pleistocene are approximate. Fault slip rates are based on the vertical displacement of middle Pleistocene deposits and the youngest middle Pleistocene time of about 130,000 B.P. We consider the average slip rates presented in this report to be maximum values because the displacements used in our estimates are for faulted middle

Pleistocene deposits that may be more than 130,000 years old. To estimate the ranges of the average recurrence intervals between large ruptures, we estimated the number of large, approximately 3- to 6.5-ft (1- to 2-m), single-event ruptures that could have displaced middle Pleistocene deposits having stage IV calcrete horizons, and we assumed that the faulted middle Pleistocene deposits are between 250,000 and 500,000 yr old.

Several intermontane basins that we discuss are called bolsons even though they do not currently exhibit internal drainage. These basins, the Hueco, Red Light, and Presidio Bolsons, contain sediments deposited in bolson settings, and thus earlier researchers (Strain, 1964, 1966, 1971; Dickerson, 1966; Akersten, 1967; Groat, 1972) called these areas bolsons. We followed the published nomenclature of the previous researchers.

Previous Work

Much of the previous work related to Cenozoic faulting of Trans-Pecos Texas involved basic regional mapping of faults and stratigraphy but included few detailed fault descriptions. Much of the previous mapping also was focused on bedrock geology; thus, Quaternary surficial deposits for many parts of Trans-Pecos Texas are not mapped in the same amount of detail and accuracy as the older bedrock deposits. Dietrich and others (1968) and Twiss (1979) produced geologic atlas sheets (scale 1:250,000) of parts of western Trans-Pecos Texas. Regional geologic maps (scale 1:250,000) for adjacent areas of Chihuahua, Mexico, were compiled by Coordinación General de los Servicios Nacionales de Estadística, Geografía e Informatica. Regional studies that specifically illustrate Quaternary faults in our study area have been done by Morrison (1969), Muehlberger and others (1978), Woodward and others (1978), Henry and others (1985), and Sergent, Hauskins, and Beckwith, Consulting Geotechnical Engineers (1989). We recently presented brief summaries of our studies of Quaternary faulting in Trans-Pecos Texas (Collins and Raney, 1992, 1993).

Quaternary faults in the Hueco Bolson area have been identified and discussed in different amounts of detail by Bell (1963), Milton (1964), Albritton and Smith (1965), Jones and Reaser (1970), Lovejoy (1971, 1972), Harbour (1972), Seager (1980), Henry and Gluck (1981), Harkey (1985), Machette (1987a, b), Barnes and others (1989a, b), Collins and Raney (1989, 1990, 1991a, b, c), Keaton and others (1989), and Keaton (1993). Less work on Quaternary faults has been done in the Red Light Bolson, where Underwood (1963) mapped several fault strands in Quaternary–Tertiary deposits in the Texas part of the Red Light Bolson. Clutterbuck (1958), Ferrell (1958), and Haenggi (1966) mapped mostly covered faults in Quaternary–Tertiary basin-fill deposits in the southern extension of the Red Light Bolson in Chihuahua, Mexico.

In the northwest Eagle Flat Basin area, where no Quaternary faults have been mapped, Underwood (1963), Albritton and Smith (1965), and King (1965), mapped the geology at scales of 1:48,000 and 1:62,500. Several faults in Quaternary–Tertiary deposits were mapped in the southeast Eagle Flat Basin and Green River Basin areas by Braithwaite (1959), Bridges (1959), Dasch (1959), Frantzen (1959), Twiss (1959), and Underwood (1963). Quaternary faults separating the west edge of the Lobo Valley Basin from the Van Horn Mountains and Sierra Vieja were mapped by Braithwaite (1958), Frantzen (1958), Bridges (1959), Dasch (1959), Twiss (1959), and Belcher and others (1977). Muelhberger and others (1985) discussed some of the scarp and displacement characteristics of these faults at the base of the Van Horn Mountains and Sierra Vieja, and they reported Quaternary displacements up to 23 ft (7 m). Hay-Roe (1957) mapped covered faults on the east margin of the Lobo Valley Basin. Quaternary faults within the Wild Horse Flat and Salt Basins were identified by King (1948, 1965), Belcher and others (1977), and Goetz (1977, 1980). Wood (1968) mapped covered faults in Quaternary deposits at the eastern margin of the Wild Horse Flat Basin.

This report does not discuss Quaternary faults of the Presidio Bolson (Groat, 1972; Henry and others, 1985) because those faults are more than 78 mi (125 km) south-southeast of the proposed repository. Some Quaternary faults in West Texas may have characteristics similar to faults in nearby New Mexico. Many investigations of Quaternary faults in New Mexico have

been conducted in more detail than most previous studies of Trans-Pecos Texas Quaternary faults. Some of the New Mexico fault studies report results of mapping, scarp analyses, and fault-displacement analyses (Machette, 1978a, b, 1982, 1987, 1988; Seager, 1981; Personius and Machette, 1984; Gile, 1987; Menges, 1987, 1990; Beehner, 1990; Kelson and others, 1993). Seismicity of the Trans-Pecos Texas region, including the 1931 Valentine earthquake that had a 6.4 magnitude, was discussed by Sellards (1932), Byerly (1934), Sanford and Toppozada (1974), Dumas (1980), Dumas and others (1980), Reagor and others (1982), Doser (1987, 1990), and Davis and others (1989).

GEOLOGIC SETTING

The desert Trans-Pecos Texas region surrounding the Eagle Flat study area (fig. 1) consists of the broad Diablo Plateau and a series of mountain ranges and adjacent basins that are the result of normal faulting that probably occurred in the last 24 mya (Henry and Price, 1985, 1986). Bedrock exposed in the mountain ranges and in the plateau consists of rocks that record the long geologic history of the region (Henry and Price, 1985; Muehlberger and Dickerson, 1989; Raney and Collins, 1993). Precambrian rocks show evidence of sedimentation, magmatism, metamorphism, and deformation prior to deposition of overlying Paleozoic strata. Paleozoic limestones indicate marine sedimentation. In the late Paleozoic the Ouachita-Marathon orogenic event produced a belt of strongly deformed Paleozoic strata across the region and structural highs, such as the Diablo Platform, were uplifted in the foreland of the Ouachita-Marathon belt. Many northwest-trending features have been related to a regional structural zone called "the Texas Lineament" (Muehlberger, 1980), which strikes across Trans-Pecos Texas. Intermittent deformation has occurred along at least parts of the Texas Lineament from the Precambrian to the present (Horak, 1985; Muehlberger and Dickerson, 1989), but major activity probably occurred during the Precambrian and the late Paleozoic. Mesozoic rocks comprise Jurassic(?) evaporites and overlying, dominantly marine Cretaceous deposits. These

Mesozoic rocks were deposited in a deep sedimentary basin, the Chihuahua Trough, which developed during the Jurassic Period in westernmost Trans-Pecos Texas and in Chihuahua, Mexico (DeFord and Haenggi, 1971; Henry and Price, 1985). Subsequent Laramide thrusting displaced Cretaceous rocks northeastward, perhaps along a décollement zone of Jurassic(?) evaporites, and produced northwest-trending thrust faults, folds, and monoclines along the northeast margin of the Chihuahua Trough (Gries and Haenggi, 1971; Gries, 1980; Henry and Price, 1985). The timing of Laramide deformation is not closely constrained, but it began no earlier than the Late Cretaceous, perhaps 80 mya (Wilson, 1971). Laramide thrust-faulting and folding appears to have ceased by about 50 mya (Price and Henry, 1985), and Laramide compressive stress appears to have waned by about 30 mya (Price and Henry, 1984; Henry and Price, 1989).

Volcanic rocks exposed throughout the Trans-Pecos region are the result of volcanic activity that occurred from 48 to 17 mya. Most of this volcanism was between 38 and 28 mya (Henry and Price, 1984, 1985; Henry and McDowell, 1986; Henry and others, 1986). Much of the volcanism in Trans-Pecos Texas occurred while the area was under regional east-northeast compression as Laramide deformation waned (Price and Henry, 1984; Henry and Price, 1985).

A transition to regional extension occurred about 30 mya, and subsequent normal faulting related to Basin and Range extension was well underway by about 24 mya (Henry and Price, 1985, 1986; Stevens and Stevens, 1985). This late Cenozoic normal faulting had a major role in the development of the present mountain ranges and basins of the region. Basin and Range faulting and related sedimentation, and magmatism in Trans-Pecos, Texas, and southern New Mexico have been episodic (Seager and others, 1984; Henry and Price, 1985; Stevens and Stevens, 1985; Mack and Seager, 1990). Precise times of accelerated fault movement and sediment deposition in most of the basins of the study area are unknown. In Trans-Pecos Texas, periods of accelerated fault movement and sediment deposition in structural troughs may have occurred 24 to 17 mya, about 10 mya, and after 7 mya (Stevens and Stevens, 1985, their fig. 4). Similar periods of deformation within the southern Rio Grande rift in southern New Mexico

were also reported by Seager and others (1984), Morgan and others (1986), and Mack and Seager (1990). In Trans-Pecos Texas, field data indicate that early regional extension was oriented east-northeast, and later extension was oriented northwest (Henry and Price, 1985; Price and Henry, 1985), but the time of this shift has not been well established. A similar change in stress-field orientation occurred in other parts of the Rio Grande rift and Basin and Range province about 10 mya (Henry and Price, 1985; Aldrich and others, 1986; Morgan and others, 1986).

During the Cenozoic, the fault-block mountains shed great amounts of sediment into the adjacent basins, partially filling them and constructing broad alluvial slopes, alluvial fans, and bajadas that surround the mountain ranges. The westernmost basin of Trans-Pecos Texas, the Hueco Bolson, also was filled with great amounts of sediment during the Pliocene that were derived from the northwest and were transported by the ancestral Rio Grande (Strain, 1971). The Cenozoic basin fill represents deposition in different settings, including alluvial fan, lacustrine, fluvial, and eolian. Some of the basins also may contain volcaniclastic deposits. The Cenozoic basin-fill stratigraphy for the basins has been studied previously in varying amounts of detail, and the stratigraphy of specific basins is briefly discussed later in this report.

Geophysical investigations and borehole data (Gates and others, 1980; Keller and Peeples, 1985) indicate that the basins have different thicknesses of basin-fill deposits (fig. 2). It is likely that the basins have had different structural histories. Sediment thicknesses in the basins may reflect different sedimentation rates that were probably at least partly influenced by faulting rates. Cenozoic slip rates of faults within individual basins also have varied (Collins and Raney, 1991c).

Trans-Pecos Texas is within the southeast part of the Basin and Range–Rio Grande Rift Stress Province (Zoback and Zoback, 1980, 1989). Regionally, the least principal horizontal stress direction of this province is west-northwest, although local variations in the stress field may occur (Zoback and Zoback, 1980, 1989). No in situ stress measurements of the stress field in

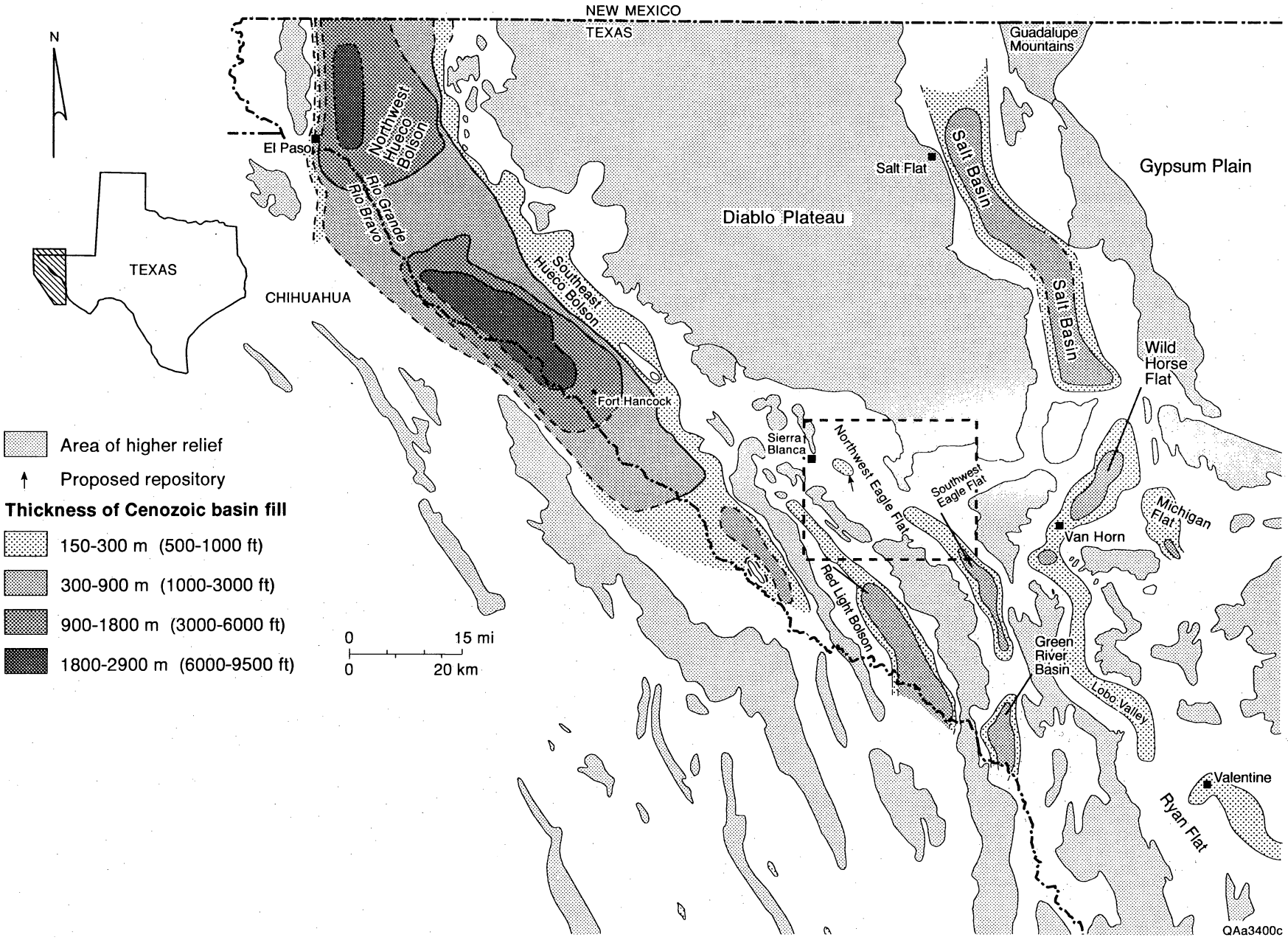

Figure 2. Location and basin-fill thicknesses of Cenozoic basins, northwestern Trans-Pecos Texas. Basin-fill thicknesses from borehole and seismic reflection data, and from Gates and others (1980) and Collins and Raney (1991c). Dashed rectangle indicates Eagle Flat study area. Arrow is approximate location of proposed repository.

the Eagle Flat study area have been made, and it is unknown how preexisting zones of crustal weakness might have affected the occurrence and geometry of Quaternary faults in the region.

Quaternary Stratigraphy

Most Quaternary deposits within the basins are associated with alluvial fan packages and arroyo terraces and alluvium. Some eolian, playa, colluvial, and fluvial deposits also exist. Many of the Quaternary faults we studied occur near basin margins where the faults cut older alluvial fans or coalescent-alluvial-fan piedmonts. Younger arroyo strath terraces that have been incised into the alluvial fans and fan piedmonts also commonly occur along the fault traces. Some faults cut older arroyo terraces. It is difficult to determine the relative ages of Quaternary deposits and landforms both within a single intermontane basin and between different basins. The Quaternary geology of Trans-Pecos Texas (fig. 3) is similar to that of southern New Mexico, where much detailed work has been done to understand the Quaternary geology, geomorphology, and calcic soils (Hawley, 1975; Gile and others, 1981; Machette, 1985). Previous studies of the Quaternary deposits and landforms of southern New Mexico serve as a necessary guide for interpreting the Quaternary geology of Trans-Pecos Texas.

Descriptions of calcic soils associated with surficial Quaternary surfaces and deposits were used to help map and compare the surficial Quaternary stratigraphy of the different basins in the Trans-Pecos. The soils also allow us to deduce the relative ages of different deposits. Calcic soils of the desert Southwest have been described in detail by Gile and others (1966, 1981) and by Machette (1985). Machette described several processes that could precipitate calcic soils, favoring a process that involves airborne $CaCO_3$ and Ca^{+2} dissolved in rainwater as the predominant sources of calcium and carbonate. The $CaCO_3$ particles are leached from the surface and upper horizons of the soil and precipitated in lower soil horizons at a depth controlled by soil moisture and texture (Machette, 1985; McFadden and Tinsley, 1985). Over time, more $CaCO_3$ precipitates in the soil horizon. Morphologic stages of $CaCO_3$ in calcic soils

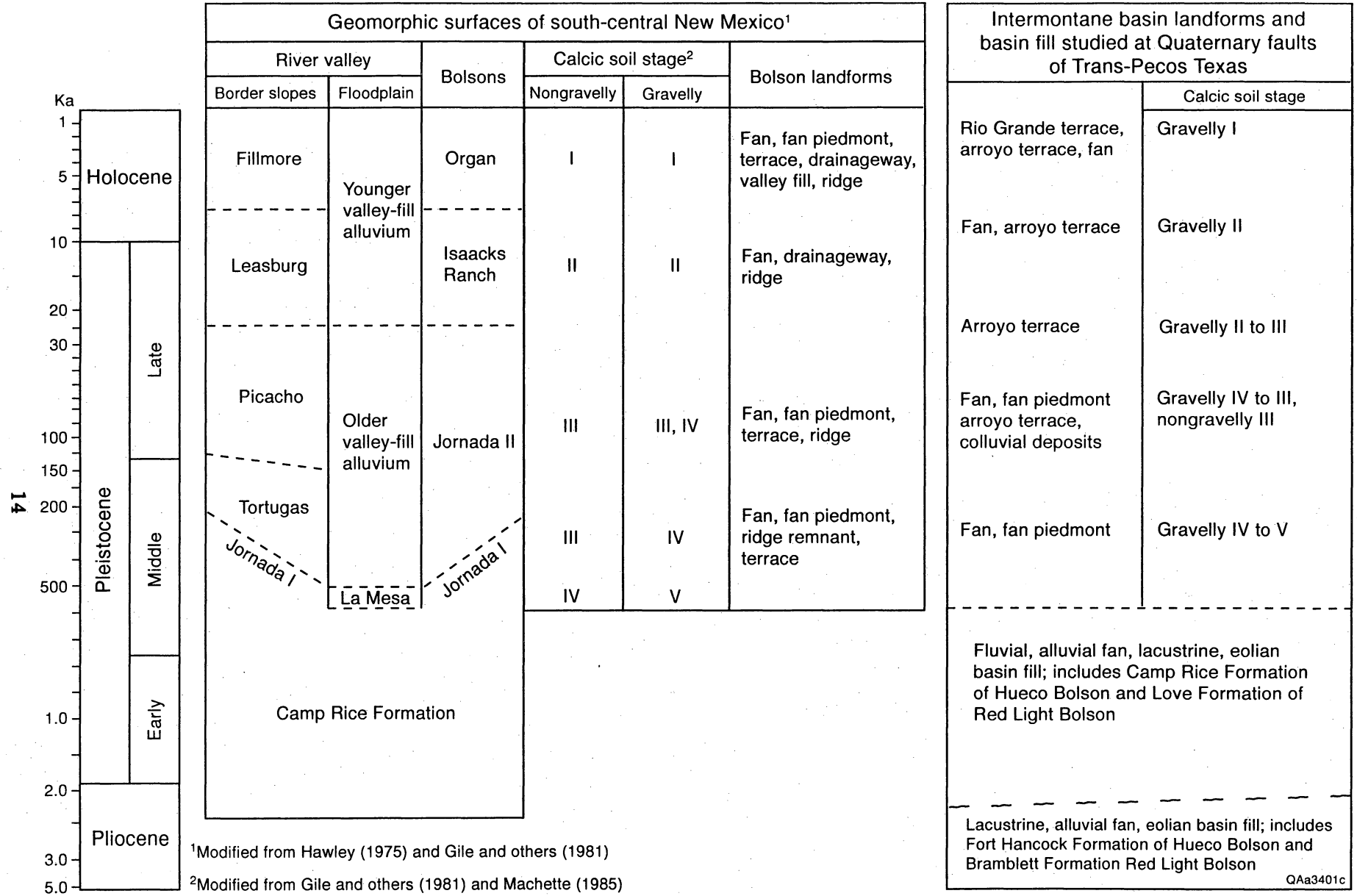

Figure 3. Quaternary stratigraphy, northwestern Trans-Pecos Texas and south-central New Mexico. We followed the Quaternary divisions and associated boundary dates presented by Morrison (1991).

and pedogenic calcretes (indurated calcic soils) that developed under arid and semiarid climates in the southwestern United States were described by Gile and others (1966) and Machette (1985). Six stages of sequential $CaCO_3$ development (numbered I to VI) are defined on the basis of physical characteristics and $CaCO_3$ distribution (Machette, 1985, his table 1). Machette (1985, his table 2) also illustrated that progressively older surficial deposits correspond to increasing stages of carbonate accumulation and morphology. In general, stage I calcic soils have thin, discontinuous $CaCO_3$ coatings on pebbles (usually on the undersides), where the gravel content is high and coatings are sparse to common. Where gravel content is low, only a few filaments of $CaCO_3$ are in the soil, or $CaCO_3$ faintly coats ped faces. Stage II calcic soils commonly have continuous coatings of $CaCO_3$ on the tops and undersides of pebbles in areas where gravel content is high, and even though some $CaCO_3$ is in the matrix, the matrix is still loose. Where the gravel content is low, $CaCO_3$ nodules may exist and the matrix is noncalcareous to slightly calcareous. Stage III calcic soils have massive accumulations of $CaCO_3$ between clasts, where gravel content is high, and where gravel content is low, the sediment matrix is firmly to moderately cemented by $CaCO_3$. Stages IV, V, and VI refer to pedogenic calcretes (indurated calcic soils). Stage IV calcretes have thin (laminae in the upper part of the horizon and have a cemented platy to weak tabular structure. Stage V calcretes have an indurated, dense, strongly platy to tabular structure. Thick laminae (0.4 inch [>1 cm]) and thin to thick pisolites may appear, and vertical faces and fractures are coated with laminated carbonate. Stage VI calcretes have multiple generations of laminae, breccia, and pisolites (Machette, 1985, his table 1).

At many of the faults in the different West Texas intermontane basins, we have estimated ages of the Quaternary deposits on the basis of field stratigraphic relationships, the degree of calcic soil development (Gile and others, 1966, 1981; Machette, 1985), and correlation with similar units in New Mexico (Hawley, 1975; Gile and others, 1981). We have mostly studied faulted and unfaulted coalescent-alluvial-fan piedmonts, alluvial fans, and arroyo and gully terraces at faults bounding the West Texas basins (fig. 3). These different deposits have calcic

soils that vary from stages I to V. For these deposits, we have estimated broad age ranges of middle Pleistocene (130,000 to 750,000 B.P.), middle Pleistocene to late Pleistocene, late Pleistocene (10,000 to 130,000 B.P.), and Holocene (present to 10,000 B.P.). In Trans-Pecos Texas, middle Pleistocene alluvial-fan surfaces having stage IV to V calcretes are probably younger than about 600,000 B.P. because an ash in the upper part of fluvial basin-fill deposits at El Paso, Texas, has been assigned as the 0.6-Ma-old Lava Creek B ash (Izett, 1981; Izett and Wilcox, 1982). The ash is stratigraphically below an extensive fan piedmont with a stage IV–V calcrete. In the Trans-Pecos Texas basins, some alluvial-fan piedmonts having stage IV calcretes about 3 ft (1 m) thick may be equivalent to the Jornada I morphostratigraphic unit of south-central New Mexico (fig. 3); thus, these landforms may be more than about 250,000 years old.

Historical Earthquakes

Most of the historical seismicity of Trans-Pecos Texas has occurred near the north-trending Salt Basin graben system and near El Paso at the west edge of the Hueco Bolson (Sanford and Toppozada, 1974; Dumas, 1980; Reagor and others, 1982; Davis and others, 1989; Doser, 1990). The largest historic event near El Paso was a Modified Mercalli (MM) intensity VI. The 1931 Valentine earthquake (Sellards, 1932; Byerly, 1934; Dumas and others, 1980; Doser, 1987), with a MM intensity VII (M = 6.4), is the largest recorded earthquake in Trans-Pecos Texas. The epicenter was located near Valentine, Texas, about 80 mi (130 km) southeast of the study area in the Ryan Flat Basin. Doser (1990) reported that it is difficult to conclusively link earthquakes in the region to specific mapped Quaternary faults because of the poor location accuracies (6 mi [10 km] or more) and lack of depth control for most earthquakes.

BASINS AND QUATERNARY FAULTS

Fourteen Quaternary faults occur within 31 mi (50 km) of the proposed Eagle Flat repository (fig. 1). The most active Quaternary faults of the region are within the Hueco and

southern Red Light Bolsons located west and south of the site, and within the Salt Graben system that encompasses the Salt, Wild Horse Flat, Michigan Flat, Lobo Valley, and Ryan Flat Basins located east of the proposed repository site. The northwest Eagle Flat, southeast Eagle Flat, and Green River basins compose a north–northwest-striking series of basins that contain only one confirmed Quaternary fault. This relationship suggests that most of the Quaternary tectonism in the region has focused along northwest- and north–northwest-trending structural zones related to intermontane basins east and west of the Eagle Flat area. The closest Quaternary fault scarp to the proposed site is 8.3 mi (13.5 km) south, in the northern Red Light Bolson.

NORTHWEST EAGLE FLAT BASIN

The northwest Eagle Flat Basin (figs. 1 and 4), the locality of the proposed repository, is a relatively shallow, internally drained basin. Most of the basin is filled by less than 500 ft (150 m) of Cenozoic gravel, sand, silt and clay (Gates and others, 1980; Jackson and Whitelaw, 1992; Jackson and others, 1993; Langford, 1993). Fault scarps do not occur in the middle Pleistocene to Holocene surficial sediments of the northwest Eagle Flat Basin. Surface bedrock geology and subsurface data from drill holes and seismic reflection data suggest that several subsurface faults may cut Cretaceous and older rocks underlying Cenozoic basin-fill sediments (Raney and Collins, 1993). It is possible that some of the older (Pliocene or older [>2.5 mya]) Cenozoic basin-fill deposits are offset, but the small maximum thickness of Cenozoic fill, small areal extent of the deep part of the basin, and the absence of fault scarps in Quaternary deposits suggest that the tectonic development and associated sedimentation of the northwest Eagle Flat Basin has been relatively inactive compared to other intermontane basins of West Texas.

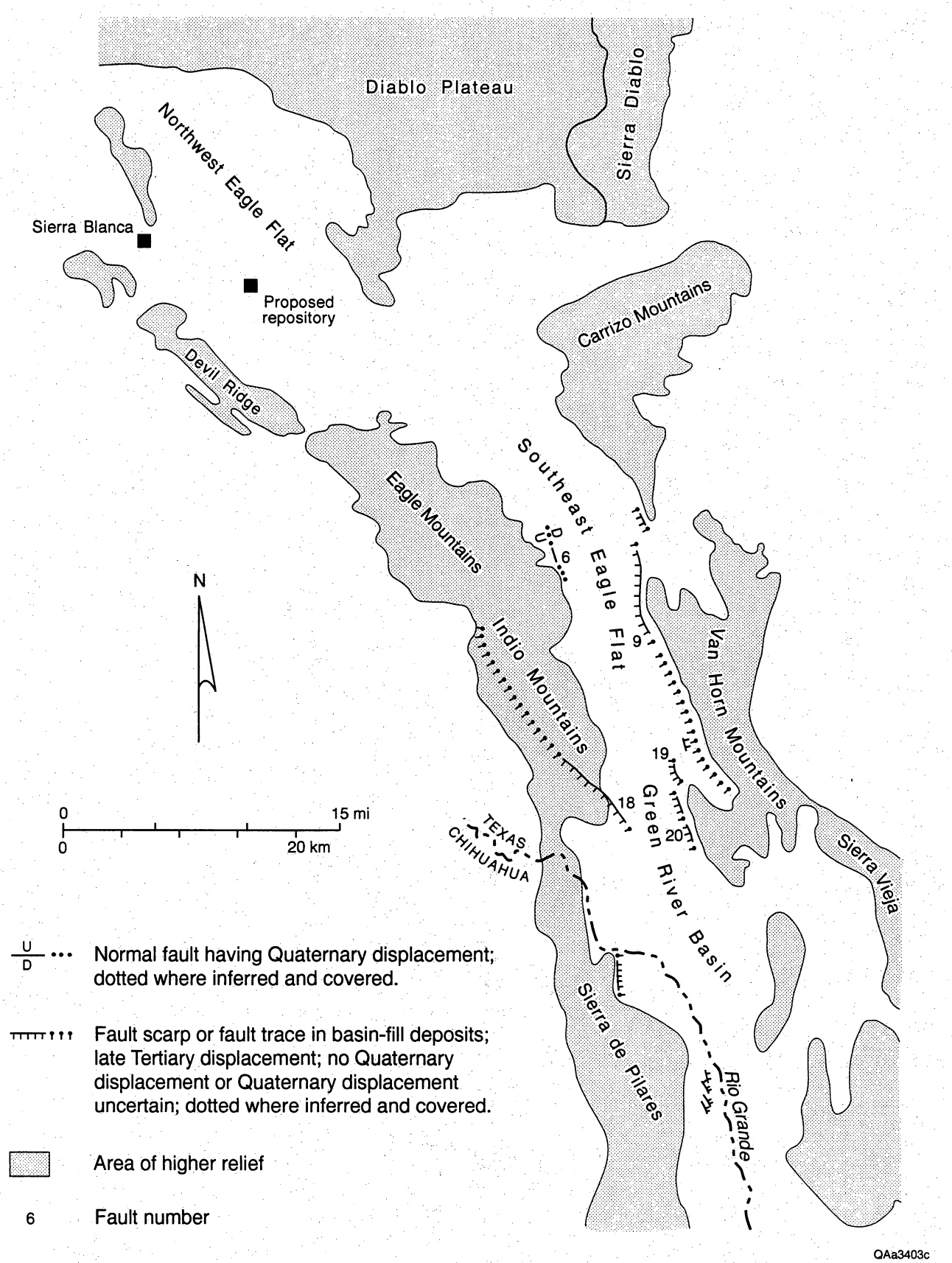

Figure 4. Quaternary and distinct late Tertiary faults, northwest Eagle Flat, southeast Eagle Flat, and Green River Basins. Geometric and displacement characteristics of the numbered faults are reported in tables A-1 and A-2.

SOUTHEAST EAGLE FLAT BASIN

The southeast Eagle Flat Basin (figs. 1 and 4) is about 25 mi (41 km) long and 3 to 8.5 mi (5 to 14 km) wide. It contains Cenozoic basin-fill deposits as thick as 2,000 ft (600 m) (Gates and others, 1980). Regional surface drainage flows southeastward and eastward into Lobo Valley. The south part of the basin is bounded by two normal faults that are expressed at the surface, the West Van Horn Mountains fault (fault 9) and the East Eagle Mountains fault (fault 6).

West Van Horn Mountains Fault

The west-dipping West Van Horn Mountains fault (fault 9, figs. 1 and 4) strikes northward at N30°W–N15°E at the base of the Van Horn Mountains and is a well expressed part of the regional Rim Rock fault zone (DeFord, 1969). Like Muehlberger and others (1978), we found no evidence of Quaternary displacement along this fault. Along most of the fault, Quaternary–Tertiary basin fill is in contact with Precambrian metasedimentary rocks, Permian limestone, and Cretaceous sandstone and limestone of the footwall. Although the contact/fault trace is sharp, no scarp is distinct. The northwestern 1.5 mi (2.5 km) of the fault trace is a gentle, dissected scarp with a slope angle of about 7°. Here the fault separates gravel deposits of unknown age on the upthrown block from Quaternary and Tertiary sand and gravel deposits on the downthrown block. A middle Pleistocene alluvial-fan piedmont with a stage IV calcrete occurs on the downthrown side of the fault. Locally the middle Pleistocene deposits are covered by younger windblown silt and sand, and also in some places the older deposits are eroded and younger fan and minor, gully and arroyo terrace sediments have been deposited. The upthrown gravel deposits form well-dissected hills with relief as much as 100 ft (30 m). Locally, on the upthrown block, a remnant geomorphic surface of unknown age exists at the scarp. Its height above the middle Pleistocene alluvial-fan piedmont on the downthrown fault block is 7.8 ft (2.4 m).

Even though this fault may not have had surface rupture during the Quaternary, we include it in this report because part of the fault does exhibit a subtle scarp in basin-fill

deposits. The length of the West Van Horn Mountains fault is 16.7 mi (27 km), and the closest distance between this fault and the Faskin Ranch reference point is 24 mi (38.5 km). The surface trace of the fault dies out northward, and there is no surface evidence of a northwest-striking fault flanking the southwest side of the Carrizo Mountains. South of the West Van Horn Mountains fault (fault 9), strands of the Rim Rock fault displace bedrock.

East Eagle Mountains Fault

On the west side of the southeast Eagle Flat Basin, a short, 0.3-mi-long (0.5-km) scarp of the East Eagle Mountains fault (fault 6, figs. 1 and 4) strikes N10°–20°W and dips eastward. This fault is inferred to be as long as 3 mi (5 km), even though most of the inferred length is covered and only a short part of the fault, 0.3 mi (0.5 km), has surface expression. The fault is on the Piñon Ranch, which is not currently accessible for ground investigations. Faulted alluvial-fan deposits are interpreted to be Quaternary and probably middle Pleistocene. This is based on study of aerial photographs and ground investigations conducted several kilometers to the north and to the east-northeast, where a fan with similar aerial-photograph characteristics and the distal part of a coalescent-fan piedmont both have a stage IV calcrete. The length of this fault was interpreted on the basis of the lack of the scarp in northern and southern alluvial-fan deposits that have the same aerial photograph characteristics as the faulted alluvial-fan deposits. The shortest distance between this fault and the Faskin Ranch reference point is 20 mi (32 km).

GREEN RIVER BASIN

South of southeast Eagle Flat is the north-trending Green River Basin (figs. 1 and 4) that is about 15 mi (24 km) long and 3 to 6 mi (5 to 10 km) wide. This basin extends into Chihuahua, Mexico, and is intersected by the Rio Grande. It has more than >2,000 ft (600 m) of Quaternary–Tertiary basin-fill deposits in its deepest part (Gates and others, 1980). Surface

drainage flows into the Rio Grande, and incision of the Rio Grande has caused increased headward erosion of arroyos and gullies that drain the Green River topographic basin. Quaternary geomorphic surfaces are well dissected and apparently have been completely eroded away in many parts of the basin; thus underlying Quaternary(?)–Tertiary basin-fill gravel, sand, and clay is commonly well exposed. The Tertiary Tarantula gravel flanks the eastern margin of the basin. DeFord and Bridges (1959) thought the Tarantula gravel resulted from Tertiary fault movement. There are subtle traces of three faults in the north part of this basin, and these faults are discussed below. Clutterbuck (1958) and Haenggi (1966) also mapped several short faults cutting Quaternary–Tertiary basin-fill deposits east of the northern Sierra de Pilares in the southern extension of the basin in Chihuahua, Mexico.

Indio Fault

The Indio fault (fault 18, figs. 1 and 4) strikes N20°–45°W, dips 65° to 75° southwest, and is composed of multiple strands. Its total length is 12.4 mi (20 km), although only the southeastern 3.7 mi (6 km) of the fault exhibits a mappable trace along a fault-line scarp where Quaternary(?)–Tertiary gravel deposits are in contact with more resistant bedrock composed of Cretaceous limestone and sandstone and Tertiary trachyte and tuff. At this southeastern part of the fault, the Indio fault flanks the northeast side of a narrow, 0.6- to 0.9-mi-wide (1- to 1.5-km) valley that may be a graben or half graben. Gravel and volcanic deposits fill the valley. Underwood (1963) thought that the gravel deposits on the downthrown block resulted from Tertiary fault movement and may be equivalent to the Tertiary Tarantula gravel, which occurs east of the Green River Basin (DeFord and Bridges, 1959). The valley drains into the Green River Basin, and the gravel valley fill appears to have undergone several periods of downcutting, leaving remnant valley-floor or terrace surfaces. The oldest of these surfaces has a stage IV calcrete and probably is middle Pleistocene. The fault is overlain by unfaulted Quaternary colluvial gravel deposits that have shed onto the valley floor from the higher

bedrock footwall block. Even though this fault has not had demonstrable Quaternary fault displacement, we included it in this study because a distinct fault-line scarp is preserved. This fault also cuts across the bedrock of the Indio Mountains and is roughly aligned with the range-front, West Eagle Mountains–Red Hills fault (fault 1) of Red Light Bolson. However, the two faults clearly have different rupture histories. The closest distance to the Faskin Ranch reference point is 31 mi (50 km).

China Canyon Fault

The China Canyon fault (fault 19, figs. 1 and 4) strikes N10°–20°W, dips eastward, and is 0.6 to 0.9 mi (1 to 1.5 km) long. The fault's surface expression is a dissected, subtle scarp, and Quaternary–Tertiary basin-fill deposits are faulted against Tertiary Tarantula gravel. Twiss (1959) mapped an inferred fault trace in the same area, although he inferred a length of 5.5 mi (8.8 km). We have not identified a scarp along most of this inferred length. This fault is included in the study because a scarp exists, although it is unknown whether the faulted basin-fill silt, sand, and gravel in this area is Tertiary or Quaternary. Thus, this fault may have been inactive since late Tertiary. The closest distance to the Faskin Ranch reference point is 32.3 mi (52 km). The China Canyon fault is en echelon to the Green River fault (fault 20, figs. 1 and 4). These faults probably have had different rupture histories because 1.5 mi (2.4 km) separates the two faults, and the Green River fault bounds a deeper part of the basin (>2,000 ft [>600 m] basin fill) than the China Canyon fault (500 ft [150 m]) basin fill on hanging-wall block).

Green River Fault

The Green River fault (fault 20, figs. 1 and 4) strikes N15°–30°W, dips west-southwest, and is 3.4 mi (5.5 km) long. It is well dissected and is composed of two main subtle fault traces that are each between 0.9 and 1.2 mi (1.5 and 2 km) long. Quaternary–Tertiary basin-fill deposits are faulted against Tertiary Tarantula gravel (Twiss, 1959). Like the China Canyon fault, it is

unknown whether the Green River fault has ruptured since the late Tertiary. The Green River fault is included in this study because a subtle scarp exists. The closest distance to the Faskin Ranch reference point is 32.2 mi (52 km).

RED LIGHT BOLSON

The northwest-trending Red Light Bolson (figs. 1 and 5) lies southwest and south of the proposed Eagle Flat repository. The bolson, which extends across the Rio Grande into Mexico, is about 56 mi (90 km) long and 4 to 6 mi (7 to 10 km) wide. The surface drainage flows into the Rio Grande, which cuts across the southern part of the bolson. The bolson contains several down-to-the-southwest Quaternary fault scarps along its eastern margin, and one of these is the closest Quaternary fault scarp to the proposed repository. Quaternary–Tertiary basin fill is thickest, greater than 2,000 ft (600 m) thick (Gates and others, 1980), in the southeastern part of the bolson. Rio Grande incision has caused much headward erosion of arroyos and gullies draining Red Light Bolson, and thus Quaternary geomorphic surfaces and associated deposits are well dissected over much of the southern and central parts of the bolson.

Tertiary–Quaternary gravel, sand, and clay basin fill are well exposed in the southern part of the bolson. Akersten (1967) proposed two basin-fill formations, the Bramblett and Love Formations, that comprise the outcropping upper 250 ft (75 m) of basin-fill deposits. He roughly correlated these formations with the Fort Hancock and Camp Rice Formations of the Hueco Bolson (Strain, 1964, 1966, 1971) on the basis of vertebrate paleontology and sedimentology. Akersten (1967) described the Pliocene Bramblett Formation as playa clay and silt with associated sand and gravel facies. He interpreted that the Bramblett sediments were deposited in a playa setting in a closed basin. Akersten (1967) reported that the overlying Pliocene–Quaternary Love Formation represents alluvial fan and fluvial sand, gravel, and clay deposited in a basin with a through-flowing axial stream. Large slumps or landslides occur in the basin-fill deposits near the Rio Grande in the southern part of the bolson (Underwood, 1963;

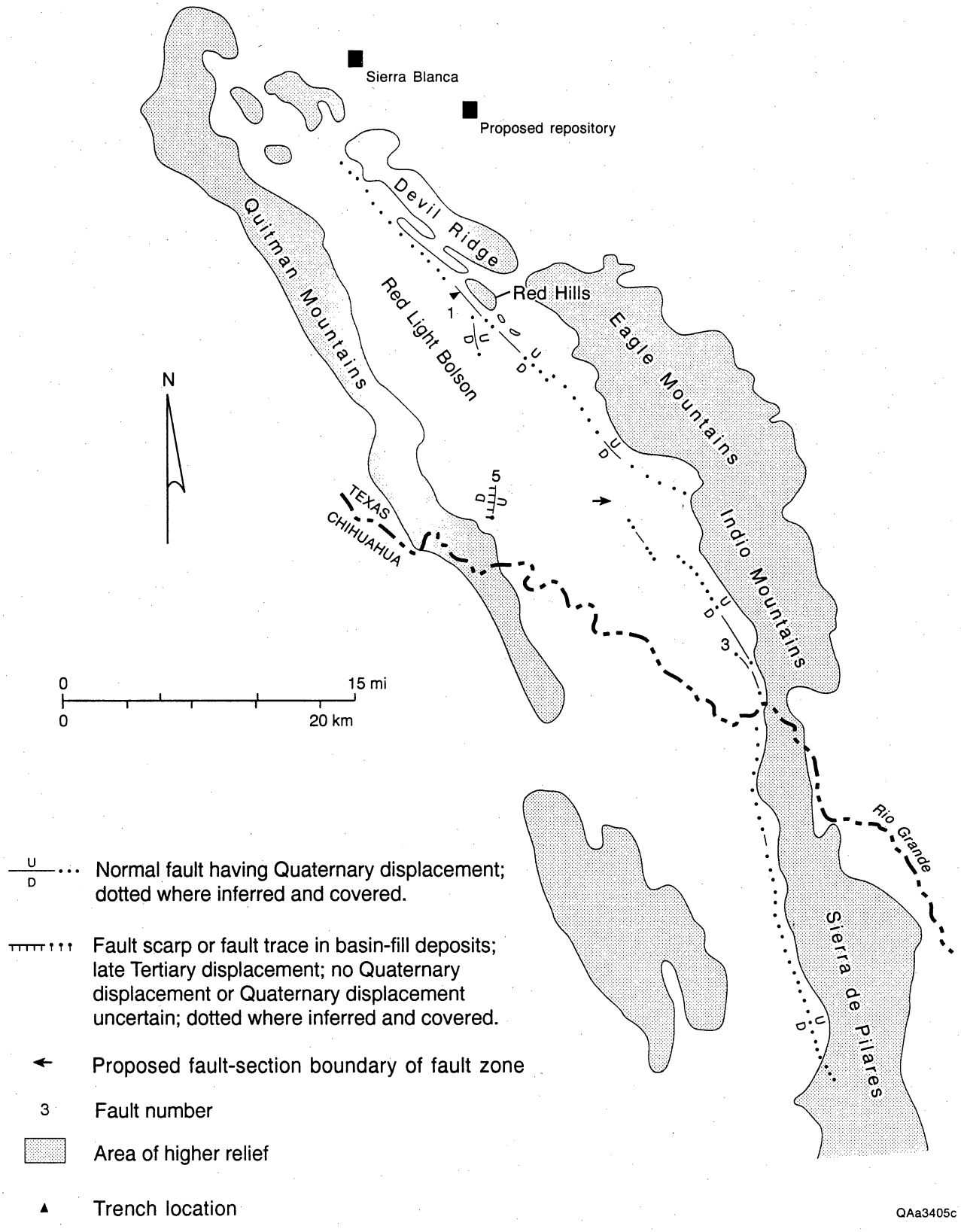

Figure 5. Quaternary faults, Red Light Bolson. Geometric and displacement characteristics of the numbered faults are reported in tables A-1 and A-2.

Thompson, 1991). Thompson (1991) postulated that the landslide that composes the Washboard Hills was triggered by a paleoseismic event, although his detailed study of this feature is not complete.

At the eastern margin of Red Light Bolson there is a Quaternary fault zone (figs. 1 and 5) that we infer to be 54 mi (87 km) long, about 20 mi (30 km) of which lies in Mexico. This fault zone is composed of at least two sections, the West Eagle Mountains–Red Hills fault (fault 1) and the West Indio Mountains fault (fault 3). Also in this bolson is another down-to-the-west fault, the Nick Draw fault (fault 5). It has a distinct surface trace, although it probably last moved in the late Tertiary.

West Eagle Mountains–Red Hills Fault

The West Eagle Mountains–Red Hills fault (fault 1, figs. 1 and 5) is expressed as a dissected 0.9-mi-long (1.5-km) scarp located west of the Eagle Mountains and two en echelon dissected scarps, 4.3 mi (7 km) and 0.6 mi (1 km) long, located west of Red Hills. We infer this fault to be as much as 24.8 mi (40 km) long on the basis of assuming that much of the fault's surface expression has been eroded or is covered along the western margin of Devil Ridge and most of the western edge of the Eagle Mountains. This fault strikes N25°–55°W. The Tertiary–Quaternary basin-fill thickness west of the Eagle Mountains is about 1,000 ft (300 m) thicker than the basin fill west of Red Hills, suggesting that different strands of the fault may have had different rupture histories.

The closest scarp to the proposed repository is 8.3 mi (13.5 km) south-southwest of the Faskin Ranch reference point. This scarp, west of Red Hills, is very subtle, with a scarp-slope angle up to only 4° and scarp heights between 4.6 and 13 ft (1.4 and 4 m). The faulted alluvial-fan deposits, probably middle Pleistocene, have a gravelly stage IV+ calcrete that is locally over 3 ft (1 m) thick. These deposits are vertically offset between 3 and 8 ft (1 and 2.5 m) along the 4.3-mi-long (7-km) scarp.

The projected trace of the West Eagle Mountains–Red Hills fault has no surface expression where it is covered by upper Pleistocene deposits with a stage II to III pedogenic calcic horizon and younger, probably Holocene deposits. This relationship suggests that these upper Pleistocene and younger deposits are not faulted.

A trench was dug across the trace of this fault at a locality west of the northern Red Hills near the closest Quaternary fault scarp to the proposed repository (fig. 5). Surficial middle Pleistocene alluvial-fan deposits are faulted at this locality. There is no distinct scarp at the trench site; however, the fault trace is well distinguished by (1) changes in vegetation across the fault where the upthrown block is sparsely vegetated mostly with sage and the downthrown block is more densely vegetated with abundant greasewood, (2) a faulted, stage IV+ calcrete horizon that is exposed only on the upthrown block in gullies that cross the fault, (3) a subtle but distinct change in the slope gradient of the fan surface across the fault, and (4) the projected strike of a 4.6-ft-high (1.4-m) scarp that occurs southeast of the trench site. The surface trace of the fault is very distinct on 1:24,000-scale aerial photographs.

The trench revealed a fault striking N25°–30°W and dipping 85° to 88° southwest (fig. 6). In the trench, the fault is expressed as of a zone of disrupted sand- and gravel-sized sediments having vertically rotated pebbles and cobbles. This zone is 2 ft (0.6 m) wide at the base of the 11.5-ft-deep (3.5-m) trench, and the fault zone narrows upward to about 0.6 ft (0.2 m) near the ground surface. On the upthrown fault block poorly sorted cobble-, pebble-, and boulder-sized limestone and sandstone gravel is capped by a 3- to 4-ft-thick (1- to 1.2-m) K soil horizon characterized by stage IV+ calcrete. As much as 6 inches (15 cm) of pebbly sand and silt overlies the calcrete. Two northwest-striking small faults and a fracture also were identified in the coarse gravel on the upthrown block.

On the downthrown fault block, three calcic soil horizons and a distinct grain-size contrast from the upthrown block exist (fig. 6). A stage III calcic horizon in mostly cobble- and pebble-sized gravel occurs about 9 ft (2.8 m) below the surface near the base of the trench. It is at least 1.6 ft (0.5 m) wide and sharply abuts the fault. The top of another gravelly stage III to IV calcic

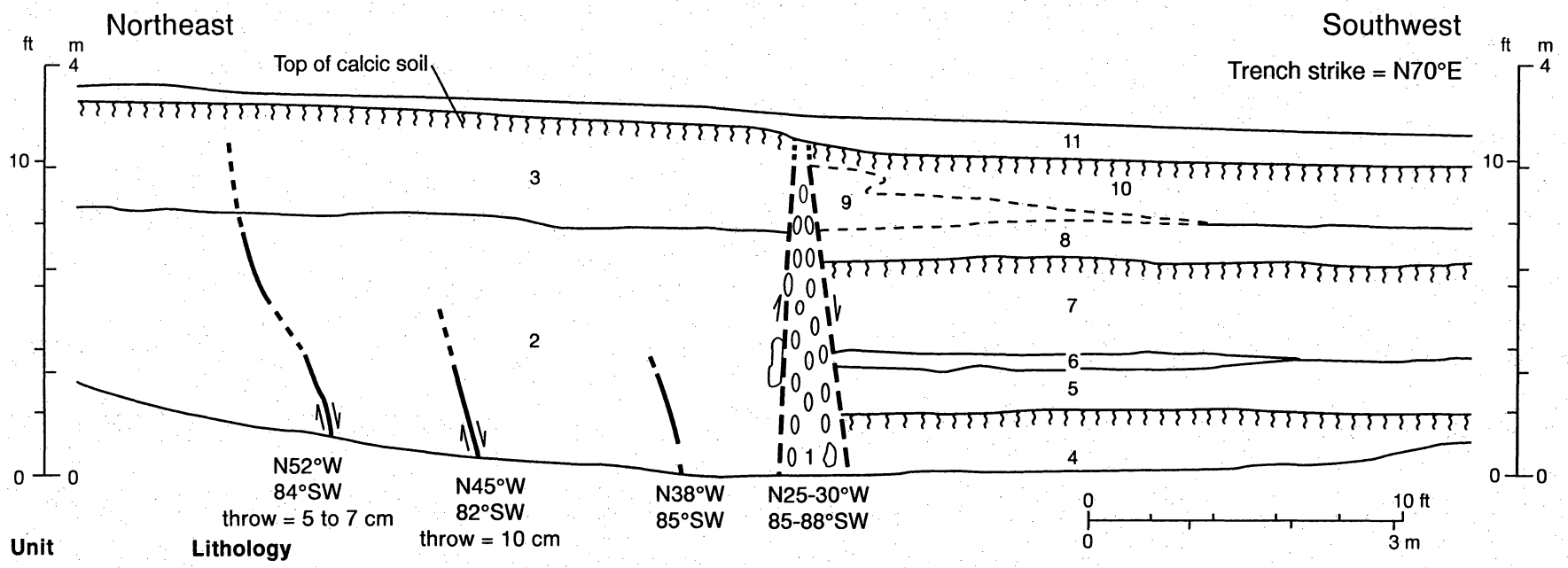

Unit **Lithology**

11 Sand and silt, some limestone and sandstone pebbles; B soil horizon; pale yellowish brown, 10YR6/2; 15 to 40 cm thick.

10 Sand, silt, pebble-sized gravel, some cobble-sized gravel; calcic soil horizon, stage IV to III morphology, locally laminated $CaCO_3$ in upper part of unit; gravel is limestone and sandstone; very light gray (N8) to white (N9).

9 Pebble- and cobble-sized gravel, sand, and silt; part of calcic soil horizon with unit 10, stage IV to III morphology; composition similar to that of units 7 and 8; gravel is limestone and sandstone; very light gray to white to very pale orange, N8 to N9 to 10YR8/2.

8 Pebble- and cobble-sized gravel, sand, and silt; some $CaCO_3$ nodules and locally high concentrations of $CaCO_3$, with sand and silt in matrix between gravel; gravel is limestone and sandstone; light brown to locally very pale orange, 5YR6/4 to 10YR8/2.

7 Pebble- and cobble-sized gravel, sand, and silt; buried calcic soil horizon, stage III to IV morphology, upper few centimeters of unit commonly composed of laminated $CaCO_3$; gravel is limestone and sandstone; very pale orange (10YR8/2) to locally light brown (5YR6/4) and very light gray (N8).

6 Sand and silt, some pebble-sized gravel; light brown (5YR6/4) to pale yellow brown (10YR6/2).

5 Pebble- and cobble-sized gravel, sand, silt, some clay; locally sandy lenses; gravel is limestone and sandstone; light brown (5YR6/4) to pale yellow brown (10YR6/2).

4 Cobble- and pebble-sized gravel, sand, silt, some clay, some boulders; locally sandy lenses; buried calcic soil horizon, stage III morphology; gravel is limestone and sandstone; mottled very light gray (N8), very pale orange (10YR8/2), and light brown (5YR6/4).

3 Pebble- and cobble-sized gravel, sand, silt, few boulders; calcic soil horizon, stage IV+ morphology; gravel is limestone and sandstone; very light gray (N8) to white (N9).

2 Cobble-, pebble-, and boulder-sized gravel, sand, silt and some clay; some sandy lenses as much as 20 cm thick; some well-sorted pebble-sized gravel lenses as much as 30 cm thick; $CaCO_3$ nodules locally; gravel is limestone and sandstone; light brown (5YR6/4) to pale yellow brown (10YR6/2).

1 Pebble-sized gravel, sand, silt, few cobbles; pebbles and cobbles are rotated; fault-zone interval; upper meter of fault zone within calcic soil horizon, upper 20 to 30 cm of fault zone is poorly defined in stage IV calcrete.

Large fault; rotated pebbles and cobbles

Small fault

Fracture

QAa3402c

Figure 6. Log of trench excavated across the West Eagle Mountains–Red Hills fault (fault 1). Trench location is west of the northern Red Hills and is shown in figure 5.

horizon is about 4.2 ft (1.3 m) from the surface. This calcic horizon is about 3 ft (0.9 m) thick, and it also sharply abuts the fault. The upper few centimeters of this horizon typically consist of laminated $CaCO_3$.

An upper, 2-ft-thick (0.6-m) stage IV to III calcic horizon on the downthrown block consists mostly of sand, silt, pebbles, and a few cobbles. The fault contact with this unit is sharp, and this unit is much more fine grained and more friable than the stage IV+ calcic horizon on the upthrown block. The top of the upper calcic horizon on the downthrown block is about 1 ft (0.3 m) lower than the stage IV+ calcic horizon on the upthrown block. At another small shallow excavation about 50 ft (15 m) south of the large trench, the relief across the fault on the upper calcic horizon is 1.6 ft (0.5 m). As much as 1.3 ft (0.4 m) of pebbly sand and silt overlies the calcic horizon on the downthrown block.

The sediments exposed in the trench (fig. 6) record evidence of at least two episodes of fault movement, sedimentation, and surface stabilization, probably since the middle Pleistocene. Vertical separations of the calcic horizons suggest that the ruptures had as much as 4.2 ft (1.3 m) of vertical slip. The relief across the fault on the uppermost calcic soil suggests a possible third rupture of up to 1.6 ft (0.5 m) of vertical slip. There has been enough time since the last rupture for dense and slightly laminated calcrete to have precipitated across the upper 8 to 12 inches (20 to 30 cm) of the fault. In the trench, fractures are not visible across the fault in the upper 8 to 12 inches (20 to 30 cm) of the calcic horizon at the surface.

The approximate average slip rate of the West Eagle Mountains–Red Hills fault since the middle Pleistocene is ≤0.02 mm/yr. We estimated the average recurrence interval, based on evidence for three large surface ruptures since the middle Pleistocene, to be about 80,000 to 160,000 yr. The Faskin Ranch reference point is as close as 6.5 mi (10.5 km) to an inferred part of the fault, which is projected beneath unfaulted cover northwest of the excavation.

West Indio Mountains Fault

The West Indio Mountains fault (fault 3, figs. 1 and 5) separates the Indio Mountains from the southern part of Red Light Bolson. This fault consists of several strands, strikes N30°–45°W, and is inferred to be up to 31 mi (50 km) long. It is interpreted to extend into Chihuahua, Mexico, along the western base of the northern Sierra de Pilares. The scarp of one strand has a slope angle of 11° to 14° and a height of as much as 10 ft (3 m). Erosion has removed much of a middle Pleistocene alluvial-fan piedmont in this area, but projection of the fan piedmont on the upthrown and downthrown fault blocks at one locality suggests as much as 30 ft (9 m) of vertical offset on these deposits. This fault strand vertically displaces middle-upper Pleistocene alluvial-fan deposits with stage IV calcrete 6 to 8 ft (1.8 to 2.5 m). Probable upper Pleistocene arroyo terrace deposits having a stage II to locally III calcic soil, are vertically offset 3 ft (0.9 m) by this strand, indicating that individual surface rupture events may have ranged from about 3 to 5 ft (1 to 1.5 m). Another fault strand has a scarp with a slope angle of 18° and height of 11.5 ft (3.5 m). Probable upper Pleistocene alluvial-fan gravel and sand deposits with boulders and cobbles have a stage II to local stage III calcic soil and are vertically offset 8 ft (2.5 m) by this fault.

We estimated the average slip rate since middle Pleistocene to be ≤0.1 mm/yr. The average recurrence interval for large surface ruptures since the middle Pleistocene is approximately 40,000 to 80,000 years. The closest distance to the Faskin Ranch reference point is 21.4 mi (34.5 km).

The West Indio Mountains and the West Eagle Mountains–Red Hills faults are interpreted to have had separate rupture histories because (1) different amounts of basin-fill thicknesses occur on the downthrown fault blocks, (2) the en echelon faults are separated by 2.5 mi (4 km), and (3) the West Indio Mountains fault displaces upper Pleistocene deposits whereas scarps of the West Eagle Mountains–Red Hills fault are absent in upper Pleistocene deposits.

Nick Draw Fault

The short, 1.5-mi-long (2.5-km) Nick Draw fault (fault 5, figs. 1 and 5) occurs in the southwest part of Red Light Bolson. This fault strikes N10°–15°E and dips west. About 0.7 mi (1.2 km) of the fault is a well expressed scarp with erosion-resistant Tertiary ignimbrite of the upthrown block in contact against Quaternary–Tertiary basin-fill deposits of the hangingwall block. Displacement during Quaternary is uncertain. Nick Draw fault's closest distance to the Faskin Ranch reference point is 18 mi (29 km).

HUECO BOLSON

The Hueco Bolson, located in westernmost Texas and Chihuahua, Mexico, is more than 105 mi (170 km) long, and most of the basin is between 15.5 and 31 mi (25 and 50 km) wide. This intermontane basin is composed of two structural basins (Collins and Raney, 1991). The northwest Hueco Basin trends northward and contains Quaternary faults that generally strike northward, whereas the southeast Hueco Basin trends northwestward and is composed of faults that strike northwestward. Cenozoic basin fill is as thick as about 8,800 to 9,800 ft (2,700 to 3,000 m) (Mattick, 1967; Ramberg and others, 1978; Wen, 1983; Collins and Raney, 1991c; Hadi and Moss, 1991). The Rio Grande flows along the axis of much of the Hueco Bolson; thus, arroyos and gullies of this intermontane basin drain into the river. Only about 100 ft (30 m) of the youngest sediments of the basin-fill sequence are exposed in outcrops. This part of the basin-fill sequence comprises the Pliocene to Quaternary Fort Hancock and Camp Rice Formations (Strain, 1964, 1966; Albritton and Smith, 1965; Riley, 1984; Stuart and Willingham, 1984; Vanderhill, 1986; Gustavson, 1991). Fort Hancock sediments were deposited in a bolson setting. These sediments are mostly lacustrine clay with some bedded gypsum, silt, and alluvial fan gravel, sand, silt, and clay, although fluvial deposits appear locally. Camp Rice sediments unconformably overlie Fort Hancock deposits. The Camp Rice is composed of sand and gravel and lesser amounts of silt and clay, and the unit represents alluvial fan, fluvial, minor lacustrine,

and floodplain deposition. Camp Rice braided-stream deposits near the basin axis were left by the ancestral Rio Grande after it developed as a through-flowing stream (Albritton and Smith, 1965). Quaternary surficial deposits mostly represent coalescent-alluvial fan, alluvial fan, arroyo terrace, Rio Grande alluvial and terrace, and eolian deposition.

Numerous Quaternary faults exist in the Hueco Bolson. Many of the faults of the northwest basin (fault zone 30, figs. 1 and 7) are covered by windblown sand and have subtle surface traces (Seager, 1980; Henry and Gluck, 1981; Collins and Raney, 1991c). However, the East Franklin Mountains fault zone (faults 28a and b, figs. 1 and 7) has distinct scarps and has been one of the most active Quaternary fault zones in the bolson. This approximately 28-mi-long (45-km) fault zone consists of two parts: (1) a 15.5-mi-long (25-km) north section that we refer to as the East Franklin Mountains fault (fault 28a) and (2) a 15.5-mi-long (25-km) south section that we call the Southeast Franklin Mountains fault (fault 28b). The Southeast Franklin Mountains fault (fault 28b) bounds the southeast part of the Franklin Mountains and probably extends into Chihuahua, Mexico. This southern fault section was not studied in detail because its surface expression has been disturbed by construction in El Paso, and it is covered by apparently unfaulted Rio Grande alluvium south of the Franklin Mountains. The northern fault section of the zone, the East Franklin Mountains fault (fault 28a), flanks most of the eastern side of the range.

Quaternary faults of the southeast Hueco Bolson (figs. 1 and 8) consist of two main zones that bound a 9- to 15-mi-wide (15- to 25-km) graben (Collins and Raney, 1991c). The Quaternary fault zone bounding the northeast margin of this graben (figs. 1 and 8) is about 65 mi (105 km) long and consists of six sections: (1) the Northwest Campo Grande fault (fault 12a), (2) the Middle Campo Grande fault (fault 12b), (3) the Southeast Campo Grande fault (fault 12c), (4) the Arroyo Diablo fault (fault 10), (5) the North Caballo fault (fault 2a), and (6) the South Caballo fault (fault 2b). Antithetic to the north and south Caballo faults is a large Tertiary fault that apparently has not moved during the Quaternary, the Schroeder fault (fault 27). The fault zone flanking the southwest margin of the Hueco Bolson, the 43-mi-long (70-km) Amargosa

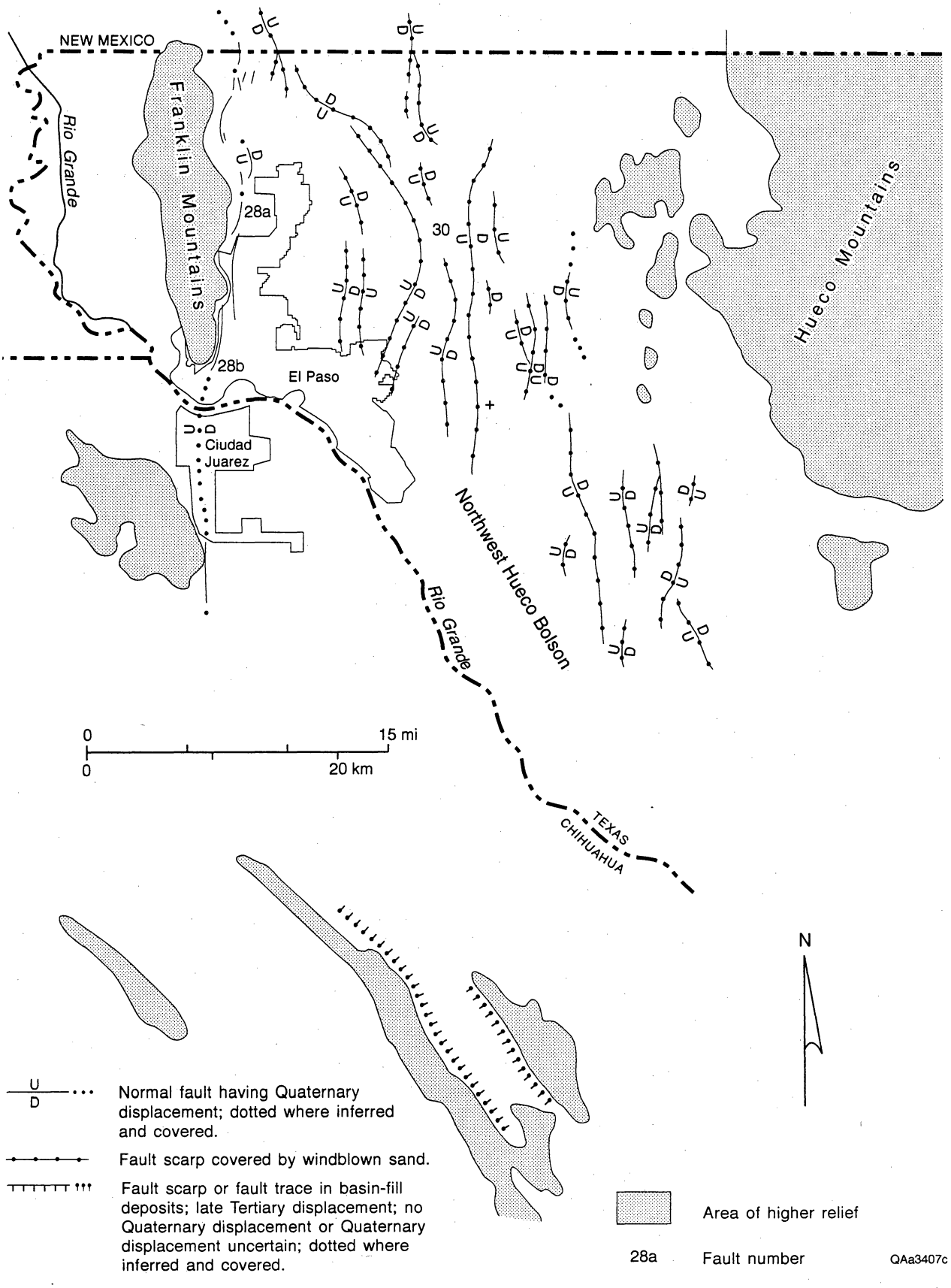

Figure 7. Quaternary faults, northwest Hueco Bolson. Geometric and displacement characteristics of the numbered faults are reported in tables A-1 and A-2.

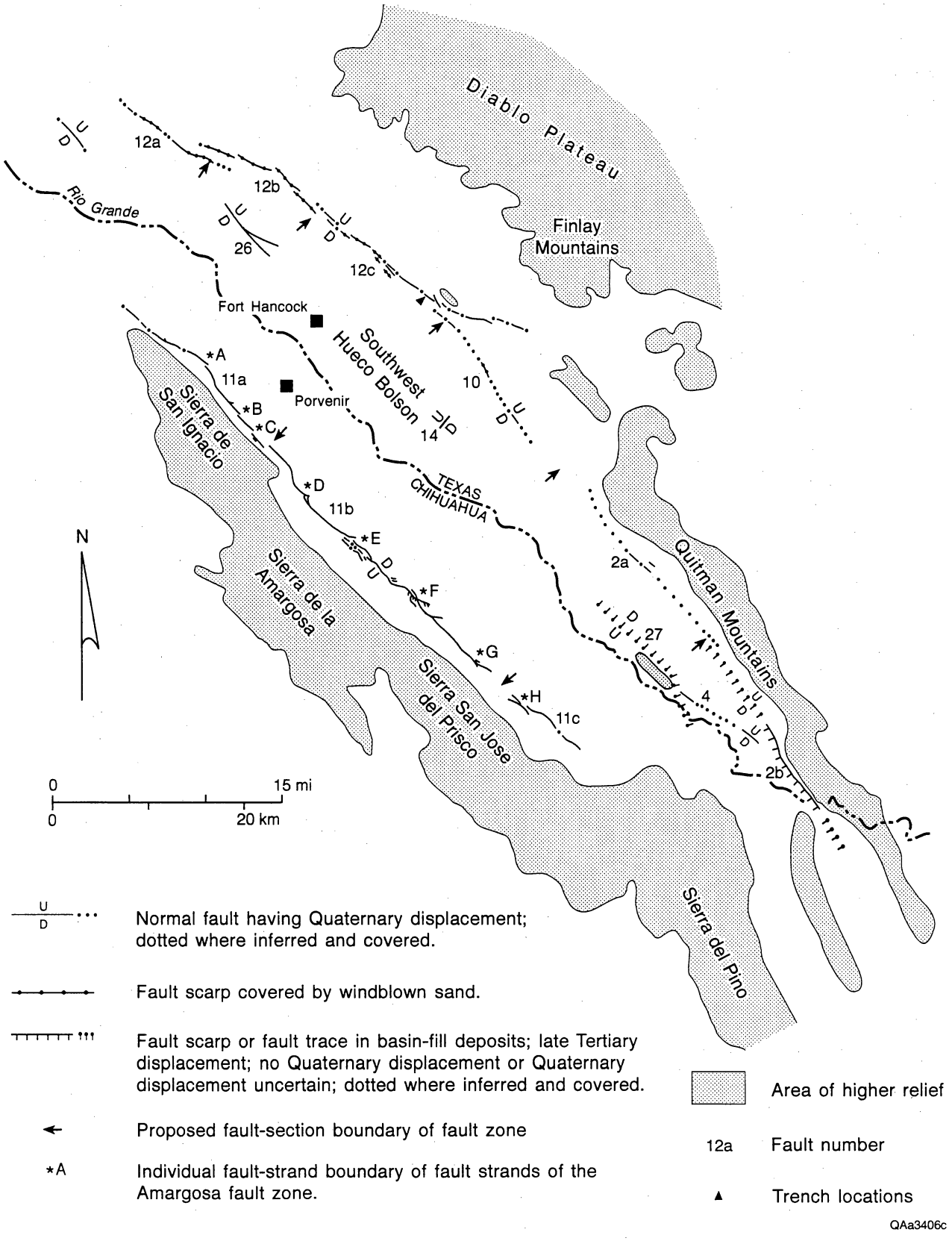

Figure 8. Quaternary faults, southeast Hueco Bolson. Geometric and displacement characteristics of the numbered faults are shown in tables A-1 and A-2.

fault zone, is composed of three sections: (1) the Northwest Amargosa fault (fault 11a), (2) the Central Amargosa fault (fault 11b), and (3) the Southeast Amargosa fault (fault 11c). Several shorter Quaternary faults also exist within the main graben of the southeast Hueco Bolson. They are the Arroyo Macho fault (fault 14), Acala fault (fault 26), and Ice Cream Cone fault (fault 4).

East Franklin Mountains Fault

The East Franklin Mountains fault (fault 28a) bounds the east flank of the Franklin Mountains and the west edge of the Hueco Bolson (figs. 1 and 7). It was called the East Boundary fault of the Franklin Mountains by Lovejoy (1971, 1972), although in more recent investigations by Machette (1987) and Collins and Raney (1991c) it was referred to as the East Franklin Mountains fault. Characteristics of this fault zone and the local geology were described by many other workers, including Richardson (1909), Sayre and Livingston (1945), Harbour (1972), Lovejoy and Hawley (1978), LeMone (1984), Machette (1987), Dyer (1989), and Collins and Raney (1991c). The East Franklin Mountains fault strikes N10°W–N10°E, dips eastward, and is composed of several fault strands (Collins and Raney, 1991c). Scarps commonly have compound-slope angles and the steepest slope angles are between 13° and 23°. Multiple rupture events have caused older Quaternary surfaces to be offset more than younger surfaces, and scarp heights generally range between 128 and 18 ft (39 and 5.5 m) because of the different ages of the faulted Quaternary surfaces along the fault trace (Collins and Raney, 1991c). The scarp heights generally do not reflect the true offset of the Quaternary surfaces because of the steep depositional slopes (commonly 5° to 6.5°) of the alluvial surfaces at the margin of the mountains and because postfaulting deposition typically covers the faulted surface on the downthrown block. In a previous study Machette (1987, his table 1, p. 44) reported scarp-slope angles between 10° and 26° and scarp heights between 6.5 and 197 ft (2 and 60 m).

Middle Pleistocene sediments, probably equivalent to the Jornada I morphostratigraphic unit (fig. 3), are vertically offset at least 105 ft (32 m). A middle to upper Pleistocene alluvial-fan surface has been vertically displaced at least 28 ft (8.5 m). An upper Pleistocene alluvial-fan surface has been vertically offset at least (14.7 to 19.6 ft) 4.5 to 6 m (Collins and Raney, 1991c). Machette (1987, p. 27) reported that sediments of late Pleistocene to Holocene age, Isaacks Ranch or younger alluvium, are offset by this fault across a 12-ft-high (3.7-m) scarp. The approximate throw during the last rupture event ranged between 5.5 and 10 ft (1.7 and 3 m) (Collins and Raney, 1991c). Machette (1987, p. 27) suggested that the youngest scarps along the East Franklin Mountains fault are early Holocene or late Pleistocene, about 10,000 to 5,000 yr old, on the basis of scarp morphology.

The approximate average slip rate since middle Pleistocene is ≤0.25 mm/yr. The average recurrence interval for large surface ruptures since middle Pleistocene is roughly estimated to be about 15,000 to 30,000 yr. Ongoing detailed investigations of this fault by Keaton (1993) may provide a more precise evaluation of the recurrence interval for this fault. The East Franklin Mountains fault is 85 mi (138 km) from the Faskin Ranch reference point and is included in this report because it has been one of the most active Quaternary faults in Trans-Pecos Texas.

Campo Grande Fault Zone

The Campo Grande fault zone (faults 12a, 12b, and 12c, figs. 1 and 8) is a 28-mi-long (45-km) series of faults that bound the northeast side of the Hueco Bolson (Collins and Raney, 1990, 1991a, b, c). This zone lies approximately midway between the Rio Grande and Diablo Plateau margin and is composed of en echelon fault strands that are 0.9 to 6 mi (1.5 to 10 km) long and that have strikes of N25°–75°W. Dips are between 60° and 89° southwest, and grooves on fault planes indicate mostly dip-slip movement. Subsurface studies indicate that the surface

trace of the Campo Grande fault zone represents three en echelon subsurface fault sections, the northwest, middle, and southeast Campo Grande faults (Collins and Raney, 1991a, c).

The northwest Campo Grande fault (fault 12a) is 13 mi (21 km) long. Its scarp is mostly covered by windblown sand, although at one locality the throw across middle Pleistocene deposits is about 46 ft (14 m). The average slip rate since middle Pleistocene is estimated to be ≤0.1 mm/yr. The average recurrence interval for large surface ruptures since middle Pleistocene is about 35,000 and 70,000 yr. This fault's closest distance to the Faskin Ranch reference point is 45 mi (72 km).

The middle Campo Grande fault (fault 12b) is 13 mi (21 km) long. Windblown sand covers the entire surface expression of this fault section; thus, displacement of Quaternary surfaces is unknown. This fault's closest distance to the Faskin Ranch reference point is 40 mi (64 km).

The southeast Campo Grande fault section (fault 12c) is the best surface expression of the zone (Collins and Raney, 1990, 1991a, b, c). The heights of scarps for this fault section range between 5 and 37 ft (1.5 and 11.5 m) and scarp slopes are 4° to 17°. Middle Pleistocene coalescent-fan piedmont deposits having a stage IV to V calcrete are vertically offset as much as 32 ft (10 m). Middle to upper Pleistocene gravelly arroyo-terrace deposits having a stage III to IV calcic soil are vertically offset as much as 10 ft (3 m). Younger upper Pleistocene arroyo-terrace deposits having a stage II calcic horizon are unfaulted. On the downthrown block of one surface fault strand, faulted nongravelly calcic soil horizons (1.6 to 3 ft [0.5 to 1.0 m thick]; stage III) that have vertical separations of 3 to 6.5 ft (1 to 2 m) indicate at least five episodes of displacement, deposition, and surface stabilization since the middle Pleistocene. Maximum vertical offsets during single faulting events have been as much as 6.5 ft (2 m), judging from the vertical separations of these faulted, calcic soil horizons. Maximum vertical offset during the last faulting event was about 3 to 5 ft (1 to 1.5 m). The approximate average slip rate for large surface ruptures since middle Pleistocene is approximately 50,000 to 100,000. The Campo Grande fault's closest distance to the Faskin Ranch reference point is 26 mi (42 km).

Arroyo Diablo Fault

The 9.3-mi-long (15-km) Arroyo Diablo fault (fault 10, figs. 1 and 8) also bounds the northeastern margin of the southeast Hueco Bolson and is located about 3 to 4 mi (5 to 6 km) south of the Finlay Mountains. This fault, previously studied by Collins and Raney (1991c, their fault 10), strikes N30°–60°W, and in outcrops it dips about 60° to 85° southwestward. Much of the trace of the Arroyo Diablo fault is covered by unfaulted sediments of late Pleistocene and Holocene age. Where a scarp is preserved on a middle Pleistocene coalescent-fan piedmont having stage IV to V calcrete, the scarp is commonly covered by windblown sand. The most distinct, uncovered scarp has heights between 5.5 and 8 ft (1.7 and 2.5 m). This scarp has compound slopes that have angles as much as 15° at the steepest part of the scarp. Middle Pleistocene deposits having stage IV to V calcrete are displaced vertically as much as 3 m (10 ft). The approximate vertical displacement on the Arroyo Diablo fault during the last surface rupture was about 2 ft (0.6 m), assuming that the steep parts of compound scarps reflect the latest single rupture event. The average slip rate since middle Pleistocene is ≤0.02 mm/yr. The average recurrence interval for large surface ruptures since the middle Pleistocene is about 125,000 to 250,000 yr. This fault's closest distance to the Faskin Ranch reference point is about 24 mi (39 km).

Caballo Fault Zone

The 29-mi-long (48-km) Caballo fault zone (faults 2a and 2b, figs. 1 and 8) bounds the west flank of the Quitman Mountains and the east margin of the southeast Hueco Bolson. Jones and Reaser (1970) named a fault strand flanking the southern Quitman Mountains the Caballo fault, and Collins and Raney (1991c) described the possible northwest extension of the fault. The fault zone is composed of two sections, a North Caballo fault (fault 2a) and a South Caballo fault (fault 2b). Both sections strike N35°–55°W and dip southwest. Most of the fault zone is difficult

to identify in the field and on aerial photographs because of erosion of the Quaternary surficial sediments and geomorphic surfaces.

Most of the 13.6-mi-long (22-km) North Caballo fault (fault 2a) is inferred (figs. 1 and 8). A 1.5-mi-long (2.5-km) well-dissected topographic scarp is postulated to be a fault scarp, although it has not been excavated. Locally this scarp has a compound slope angle, and its total height is 34 ft (10.5 m). The steep part of the compound slope is 15°. Along the scarp, a middle to upper Pleistocene fan surface may be displaced vertically 23 ft (7 m). The scarp is not expressed in younger upper Pleistocene deposits. Projection of a dissected middle Pleistocene alluvial-fan surface (stage IV–V calcrete) across the inferred fault trace suggests as much as 78 ft (24 m) of vertical offset, although erosion of sediments makes precise measurement difficult (Collins and Raney, 1991c). The approximate amount of vertical offset during the last surface rupture was about 5.5 ft (1.7 m), assuming that the steep part of the compound scarp reflects the latest single rupture event. The average slip rate since middle Pleistocene is ≤0.2 mm/yr. The average recurrence interval for large surface ruptures since middle Pleistocene is estimated to be 20,000 to 40,000 yr. The North Caballo fault's closest distance to the Faskin Ranch reference point is 14.3 mi (23 km).

Much of the 16-mi-long (26-km) South Caballo fault cuts Quaternary(?)–Tertiary basin-fill sediments cropping out on both sides of the fault or the fault has displaced basin-fill deposits against Cretaceous bedrock. At one locality the fault has a steep dip of about 70° to 80° southwestward. This South Caballo fault is not expressed by a scarp on middle Pleistocene fan surfaces and does not displace colluvium that covers the base of the mountains and edge of the basin. These field observations suggest this fault has not moved at least since the middle Pleistocene. It is unknown if any faulted basin-fill deposits are early Pleistocene. The south Caballo fault's closest distance to the Faskin Ranch reference point is 15 mi (24 km).

Amargosa Fault Zone

The Amargosa fault zone (faults 11a, 11b, and 11c, figs. 1 and 8) flanks the northeast base of Sierra de San Ignacio, Sierra de la Amargosa, and Sierra San Jose del Prisco of Chihuahua, Mexico, and separates these mountains from the southwest edge of the Hueco Bolson (Collins and Raney, 1991c, their fault 14). The fault zone has a very well expressed surface trace of about 43 mi (70 km) and a regional strike of N40°–50°W. It dips northeast between 75° and 80° at the surface. The fault appears to exhibit mostly vertical offset where we studied it, although Barnes and others (1989) and Keaton and others (1989) reported grabenlike extensional features along the fault as evidence of lateral components of fault slip.

This fault zone (figs. 1 and 8) consists of three fault sections, the 13-mi-long (21-km) Northwest Amargosa fault (fault 11a), the 22-mi-long (35.5-km) Central Amargosa fault (fault 11b), and the 6.2-mi-long (10-km) Southeast Amargosa fault (fault 11c). The northwest and central faults have an en echelon boundary, whereas the boundary between the central and southeast faults is a gap (fig. 9). The Northwest Amargosa fault consists of four main, closely spaced en echelon strands that step to the right (figs. 8 and 10a, b, c). The en echelon boundary between the northwest and central sections is a 0.4-mi-wide (0.7-km) left step (fig. 9a). The Central Amargosa fault section consists of five main fault strands and many subsidiary strands. Along this fault section, the main northwestern strands step to the right and the main southeastern strands step to the left (figs. 8 and 10d, e, f, g). Possible ramps or structural bridges are expressed at two of the closely en echelon fault boundaries (fig. 10). We postulate that some of the faults associated within the ramp structures may exhibit slip oblique to the fault dip. The fault section boundary between the Central Amargosa and Southeast Amargosa faults is a 2.2-mi-wide (3.5-m) gap (fig. 9b). The Southeast Amargosa fault comprises two main, left-stepping en echelon strands (figs. 8 and 10h).

The Amargosa fault zone has the most distinct fault scarps in the southeast Hueco Bolson. Scarp-slope angles are between 19° and 27°. Scarp heights range between 105 and 9 ft

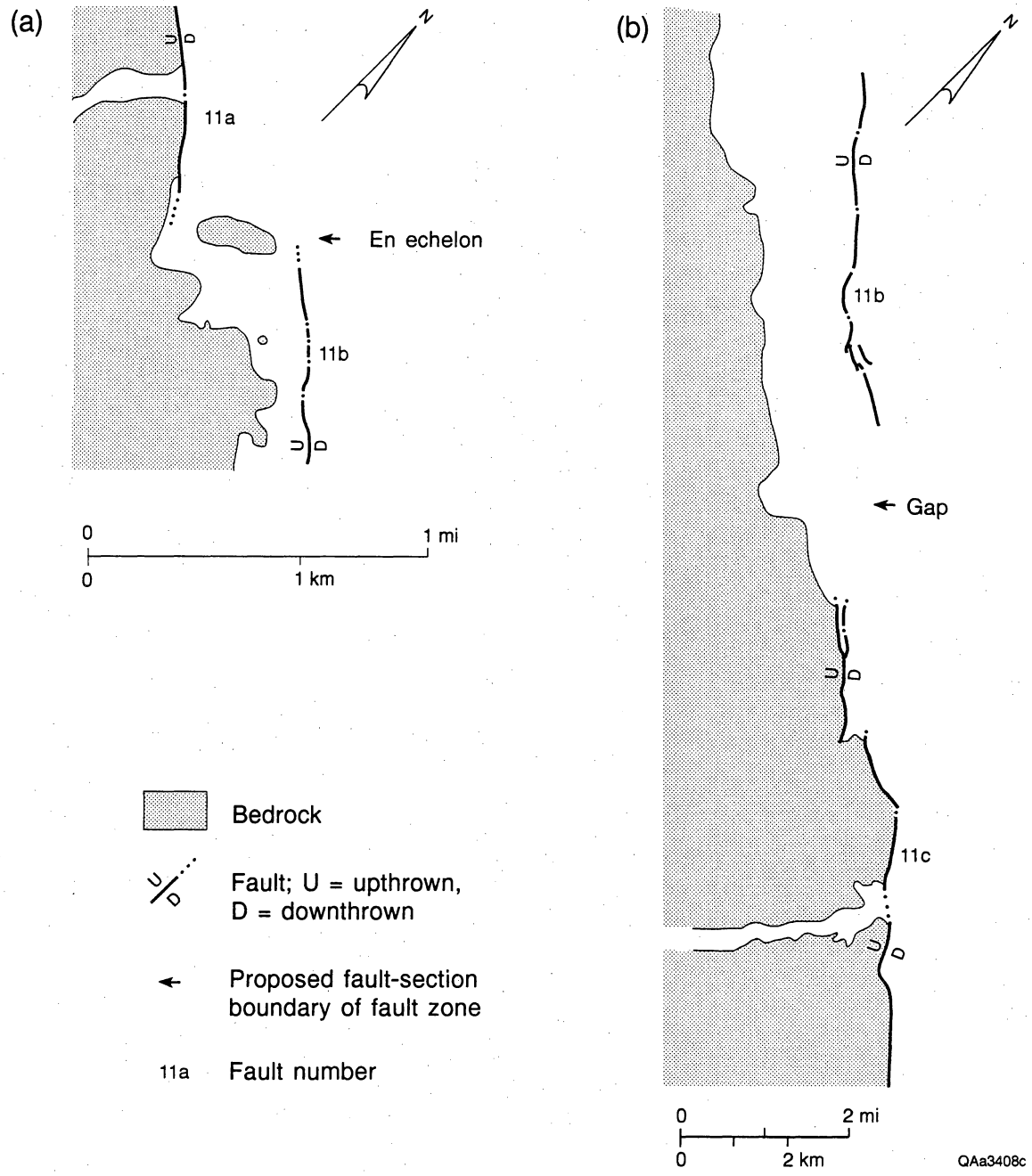

Figure 9. Section boundaries of the (a) Northwest Amargosa fault (fault 11a) and Central Amargosa fault (fault 11b), and (b) Central Amargosa fault (fault 11b) and Southeast Amargosa fault (fault 11c). Locations of (a) and (b) are shown in figure 8 as arrows along the Amargosa fault zone (faults 11a, 11b, and 11c).

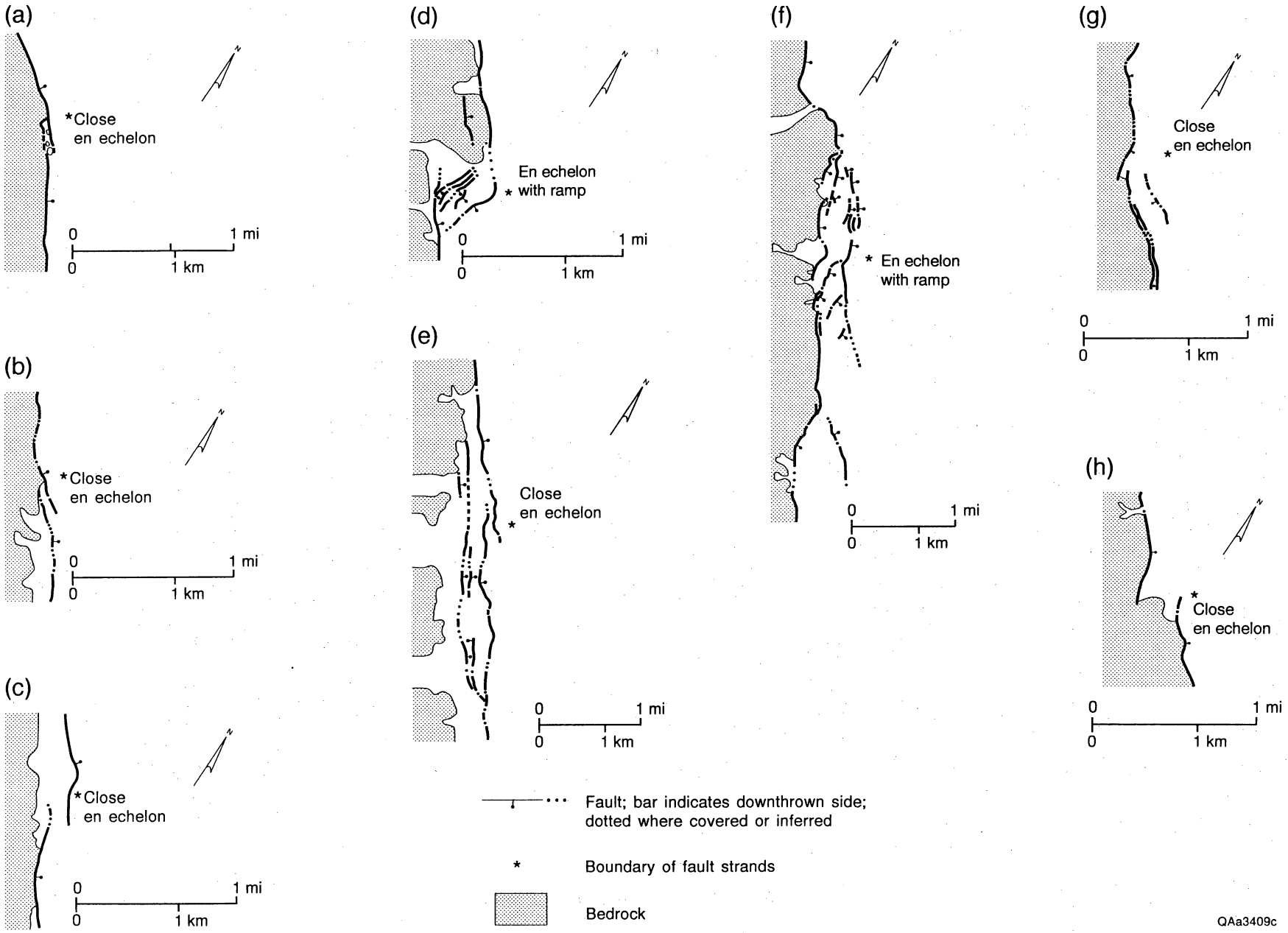

Figure 10. Fault strand boundaries along the Amargosa fault zone (faults 11a, 11b, and 11c, fig. 8). Areas (a) through (c) are along the Northwest Amargosa fault (fault 11a, fig. 8), (d) through (g) are along the Central Amargosa fault (fault 11b, fig. 8), and (h) is along the Southeast Amargosa fault (fault 11c).

(32 and 2.8 m), depending on the age of faulted sediments adjacent to the fault, because multiple ruptures have caused older Quaternary surfaces to be offset more than younger ones.

Middle Pleistocene fan-piedmont deposits having stage IV to V calcrete are offset vertically 78 ft (24 m) across the Northwest Amargosa fault (fault 11a). Middle to upper Pleistocene arroyo terrace and fan deposits having stage III to IV calcic soils are offset vertically as much as 21.3 and 19.6 ft (6.5 and 6 m) across the Northwest Amargosa and Central Amargosa faults (faults 11a and 11b, respectively). Younger upper Pleistocene Arroyo terrace and fan deposits having stage II calcic soils are displaced vertically 8.2 to 14.7 ft (2.5 to 4.5 m) across the Northwest Amargosa fault (fault 11a). Results of aerial photographic mapping suggest that young, possibly Holocene deposits, may be offset at some localities along the Amargosa fault (Collins and Raney, 1991c). The average slip rate since the middle Pleistocene is ≤0.2 mm/yr. The average recurrence interval for large surface ruptures since the middle Pleistocene is about 20,000 to 40,000 yr. The Southeast Amargosa fault is the closest fault section of this zone to the Faskin Ranch reference point. It is 25.4 mi (41 km) away. The central and northwest fault sections are 27 and 38.5 mi (43 and 62 km) from the Faskin Ranch reference point.

Acala Fault

The Acala fault (fault 26, figs. 1 and 8) strikes N40°–50°W, dips southwest, and has a surface trace of about 6.2 mi (10 km) (Collins and Raney, 1991c, their fault 7). The scarp has a single-slope angle of 9° (maximum), and the scarp is about 7.2 ft (2.2 m) high. Middle Pleistocene alluvial-fan-piedmont deposits having a stage IV to V calcrete are estimated to be displaced vertically about 59 ft (18 m). A shorter fault scarp having a surface trace of about 1.8 mi (3 km) (Collins and Raney, 1991c, their fault 8) is roughly en echelon to the longer scarp. The shorter scarp strikes N60°–70°W and dips southwest. Its scarp has a single-slope angle of about 4°, and the scarp is only about 3 ft (1 m) high. Middle Pleistocene alluvial-fan deposits having a stage IV to V calcrete are vertically offset about 13 ft (4 m). The average slip rate since the middle

Pleistocene is ≤0.2 mm/yr. The average recurrence interval for large surface ruptures since the middle Pleistocene is approximately 30,000 to 60,000 yr. The Acala fault's closest distance to the Faskin Ranch reference point is 42 mi (68 km).

Arroyo Macho Fault

The short 0.9-mi-long (1.5-km) Arroyo Macho fault (fault 14, figs. 1 and 8) strikes N30°–40°E and dips southeast (Collins and Raney, 1991a, their fault 11). Albritton and Smith (1965) measured 6.5 ft (2 m) of displacement on middle Pleistocene alluvial-fan deposits having a stage IV to V calcrete. The average slip rate since the middle Pleistocene is ≤0.01 mm/yr. The average recurrence interval for surface ruptures since the middle Pleistocene is approximately 125,000 to 250,000 yr. Arroyo Macho fault's closest distance to the Faskin Ranch reference point is 27.3 mi (44 km).

Ice Cream Cone Fault

The northwest-trending Ice Cream Cone fault (fault 4, figs. 1 and 8) strikes N15°–60°W, dips as much as 85° southwest, and has a surface trace of about 5.6 mi (9 km). This fault, described by Collins and Raney (1991c, their fault 12), appears to vertically displace middle–upper Pleistocene deposits 45 ft (13.8 m), although extensive erosion of the area makes correlation of the faulted middle to upper Pleistocene deposits difficult. Younger upper Pleistocene gravel deposits are not faulted. Recent investigation of seismic reflection data indicates that the Ice Cream Cone fault is antithetic to the Schroeder fault (fault 27, figs. 1 and 8), a larger Tertiary fault. The average slip rate since the middle to late Pleistocene is ≤0.1 mm/yr. Because data on fault displacement are sparse, the approximate average recurrence interval for surface ruptures since the middle–late Pleistocene only was estimated as greater than 15,000 yr. The Ice Cream Cone fault's closest distance to the Faskin Ranch reference point is 18 mi (29 km).

Schroeder Fault

The Schroeder fault (fault 27, figs. 1 and 8) lacks surface expression but is well defined on seismic reflection data. This fault is at least about 11.5 mi (18.5 km) long, and it strikes about N30°–50°W and dips eastward. Seismic reflection data indicate that this fault dips about 60° in the subsurface. The fault does not appear to cut Tertiary–Quaternary basin-fill deposits that are exposed in arroyos that cross the projected fault trace; thus, we postulate that the fault has not ruptured since the late Tertiary. It is possible that Quaternary displacement of the Schroeder fault (fault 27) cannot be distinguished with available outcrops. If the Quaternary Ice Cream Cone fault (fault 4) is an antithetic fault related to the Schroeder fault (fault 27), then Quaternary displacement on the Schroeder fault may also have occurred. The Schroeder fault's closest distance to the Faskin Ranch reference point is 18.3 mi (29.5 km).

LLANOS DE CHILICOTE

Llanos de Chilicote lies in Chihuahua, Mexico, southwest of the proposed Eagle Flat repository. Two faults, the West Sierra de la Lagrima fault and the West Sierra Labra fault (faults 23 and 25, respectively, fig. 1), bound mountain ranges of the Llanos de Chilicote region and have been mapped as the contact between Tertiary–Quaternary gravel and sand deposits and Cretaceous bedrock on the San Antonio El Bravo sheet (Coordinación General de los Servicios Nacionales de Estadística, 1982). We have not studied these faults using aerial photographs because we have had no access to photographs, and we have not visited the area on the ground. Thus, we do not know if fault scarps exist in this area. Surface expression and Quaternary offset of these faults is uncertain on the basis of the Gries (1979, 1980) hypothesis that Cenozoic extension in this region may have reactivated older structures and caused flowage of thick evaporite sequences and that Cenozoic extension may not be expressed as faults at the surface.

West Sierra de la Lagrima Fault

The West Sierra de la Lagrima fault (fault 23, fig. 1) has been mapped as a 41-km-long (25.4-mi) structure that strikes north-northwest at N5°–35°W and dips west (Coordinación General de los Servicios Nacionales de Estadística, 1982). This fault's closest distance to the Faskin Ranch reference point is 40 mi (61 km).

West Sierra Labra Fault

The West Sierra Labra Fault (fault 25, fig. 1) has been mapped as a 13.6-mi-long (22-km) structure that strikes north-northwest at N0°–30°W and dips west (Coordinación General de los Servicios Nacionales de Estadística, 1982). This fault's closest distance to the Faskin Ranch reference point is 40 mi (65 km).

SALT BASIN GRABEN SYSTEM

The north-trending Salt Basin graben system lies east of the proposed repository site. The graben system comprises a 124-mi-long (200-km) series of fault-bound basins that include, north to south, the Salt, Wild Horse Flat, Michigan Flat, Lobo Valley, and Ryan Flat Basins (figs. 1 and 2). The Salt Basin is greater than 62 mi (100 km) long and is 7.4 to 15.5 mi (12 to 25 km) wide; the southern part is sometimes referred to as the Salt Flat geographic area. Surface drainage of the Salt Basin is inward, and alkali flats exist on the bolson's floor. King (1965) thought that the alkali flats might be the remnants of earlier, more extensive lakes. He also recognized ridges that he thought might mark the shores of an earlier Pleistocene lake. At the edges of the Salt Basin, alluvial fans have built out from the mountains to form a relatively broad, 1- to 5-mi-wide (1.6- to 8-km) alluvial slope. King (1965) reported that alluvial-fan deposits in the basin probably have a wide age range. He also recognized that smaller fans with the steepest gradients and coarsest fanglomerate are along the part of the Sierra Diablo north of

the Baylor Mountains, where the most recent faulting has resulted in active erosion and deposition. Goetz (1977, 1980) mapped Quaternary faults and aerial-photograph lineaments in this basin and in the Wild Horse Flat Basin. She recognized that the graben is asymmetric and that the thickest basin-fill deposits are on the western margin. Tertiary to Quaternary basin-fill in the Salt Basin is greater than 2,000 ft (600 m) thick in some areas (King, 1965; Goetz, 1977, 1980; Gates and others, 1980).

Wild Horse Flat Basin lies south of Salt Basin, and it is about 18.6 mi long (30 km) and about 9.3 mi (15 km) wide. This basin receives surface drainage from Lobo Valley and Michigan Flat, and the surface drainage flows into Salt Basin. Similar to Salt Basin as well as Lobo Valley, Michigan Flat, and Ryan Flat, alluvial fans have built out from the bounding mountains into the basin and the fans coalesce into an alluvial plain. The floor of Wild Horse Flat does not contain alkali flats. Quaternary–Tertiary basin-fill deposits are thicker than 1,000 ft (300 m) in Wild Horse Flat Basin (Gates and others, 1980).

Lobo Valley Basin is south of Wild Horse Flat Basin, and the valley receives surface drainage from southeast Eagle Flat and Ryan Flat. The Lobo Valley Basin is about 34 mi (55 km) long and is 5.6 to 7.5 mi (9 to 12 km) wide. It is generally narrower than the other basins of the Salt Basin graben system. Tertiary–Quaternary basin-fill deposits are thicker than 1,000 ft (300 m) in the northern part of Lobo Valley Basin, and the basin is asymmetric with thicker Cenozoic fill along the western half of the basin (Gates and others, 1980). Ryan Flat Basin is southeast of Lobo Valley Basin. It is about 31 mi (50 km) long and about 12.4 mi (20 km) wide. Surface drainage flows into Lobo Valley. Quaternary–Tertiary basin-fill deposits in Ryan Flat Basin are thicker than 500 ft (150 m), according to Gates and others (1980).

The western side of the Salt Basin Graben system is characterized by an approximately 105-mi-long (170-km) series of Quaternary faults. Some Quaternary faults also exist along parts of the eastern side of the graben system. Many of the Quaternary faults along this system had previously been identified by Twiss (1959), King (1965), Belcher and others (1977), Muelhberger and others (1978, 1985), and Goetz (1977, 1980). We divide the long series of

west boundary faults into three main fault zones: (1) the 59-mi-long (95-km) West Salt Basin fault zone, (2) the 25-mi-long (41-km) East Carrizo Mountain–Baylor Mountain fault, and (3) the 40.3-mi-long (65-km) West Lobo Valley fault zone (figs. 1 and 11).

SALT BASIN FAULTS

The Salt Basin (figs. 1 and 11) is bounded by the West Salt Basin fault zone on the west and the Delaware Mountains fault zone on the east. Covered Quaternary faults also may flank the west side of the Guadalupe Mountains, the highest range of the region with an elevation up to 8,750 ft (2,667 m). The West Salt Basin fault zone is composed of at least four sections: the Dell City fault (fault 29), East Flat Top Mountains fault (fault 21), the North Sierra Diablo fault (fault 22), and the East Sierra Diablo fault (fault 8).

Dell City Fault

The Dell City fault (fault 29, figs. 1 and 11) strikes N45°–65°W and dips northeastward. It is about 11.8 mi (19 km) long. It is unknown if this fault has had Quaternary movement. The fault is covered and the fault's trace is identified by the contact between Permian limestone and Quaternary alluvium. This fault's closest distance from the Faskin Ranch reference point is 45 mi (72 km).

East Flat Top Mountains Fault

Thirty-four miles (53 km) north-northeast of the Faskin Ranch reference point, the East Flat Top Mountains fault (fault 21, figs. 1 and 11) bounds the west side of the Salt Basin. This 14.2-mi-long (23-km) fault strikes northward at N25°W–N5°E and dips toward the east. Aerial photograph studies indicate that scarps between 0.3 and 1.2 mi (0.5 and 2 km) long are present, although about 80 percent of this zone is covered or inferred. One subtle scarp located

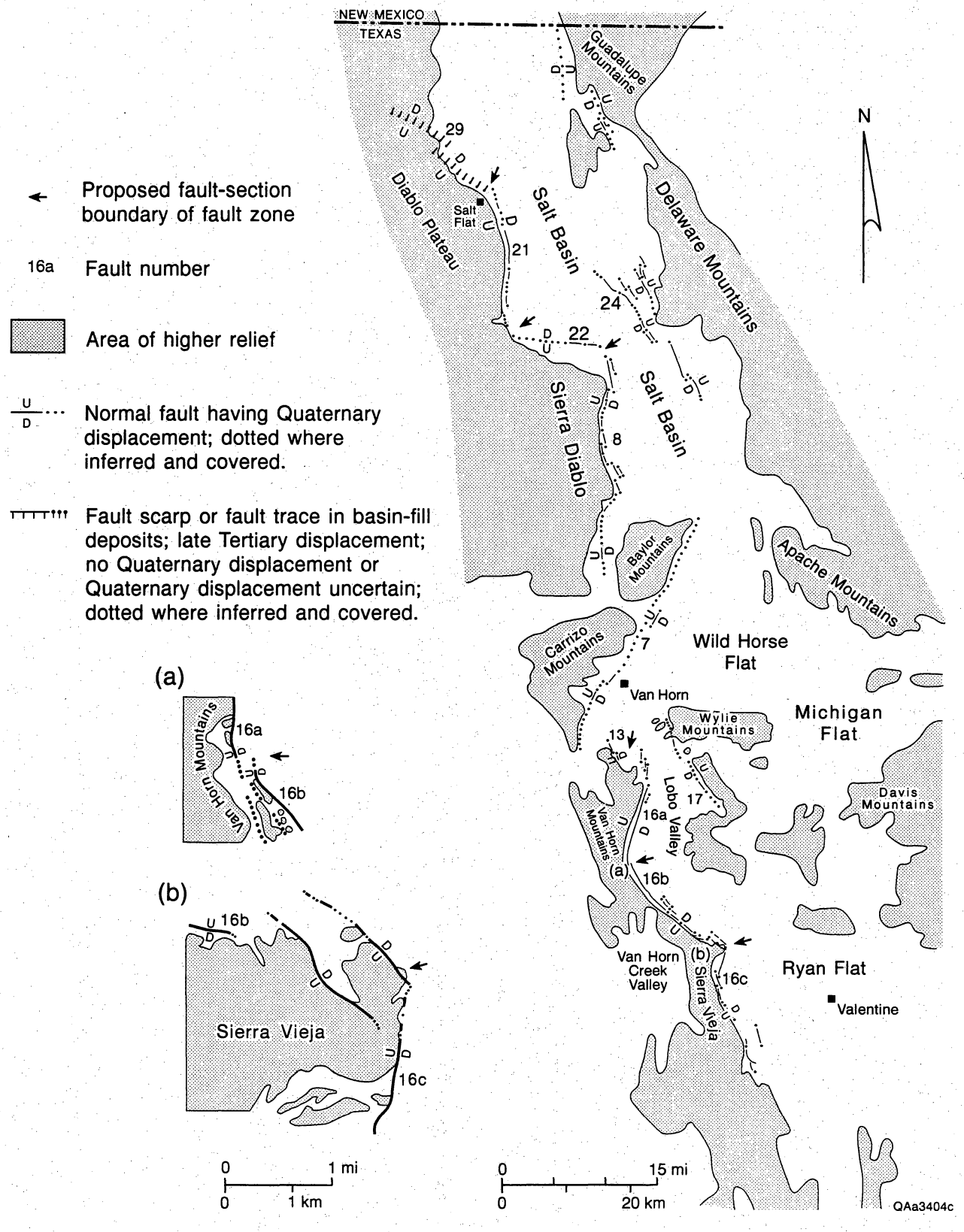

Figure 11. Quaternary faults, Salt Basin graben system. Boundary of Neal fault (fault 16a) and Mayfield fault (fault 16b) shown in inset map (a). Boundary of Mayfield fault (fault 16b) and Sierra Vieja fault (fault 16c) shown in inset map (b). Geometric and displacement characteristics of numbered faults shown in tables A-1 and A-2.

at the northern part of this fault has a scarp-slope angle of 3° and height of about 8 ft (2.5 m). The faulted surficial sediments at this locality are unconsolidated, lack a well-developed calcic soil horizon, and probably are Holocene or late Pleistocene. Offset of the faulted geomorphic surface is about 5 ft (1.5 m).

North Sierra Diablo Fault

The North Sierra Diablo fault (fault 22, figs. 1 and 11) strikes westward at N75°–85°W, dips north, and separates the north part of Sierra Diablo from the Salt Basin. About 70 percent of the 8.3-mi-long (13.5-km) fault is covered or inferred, although a 2.5-mi-long (4-km) scarp occurs at the fault's eastern end. This fault's closest distance to the Faskin Ranch reference point is 33.5 mi (54 km).

East Sierra Diablo Fault

The 23-mi-long (37-km) East Sierra Diablo fault (fault 8, figs. 1 and 11) strikes northward at N10°W–N20°E, dips toward the east, and bounds the eastern base of Sierra Diablo. This fault is composed of a series of about 11 en echelon fault strands, and about 60 percent of the fault's length is covered or inferred. The longest continuous scarp, located at the northern part of the East Sierra Diablo fault, is 3 mi (5 km) long, and it has a scarp-slope angle of 8° and height of 6 ft (1.8 m). At the northern part of this longest scarp, the faulted surficial sediments consist of an upper, unconsolidated, 6.5-ft-thick (2-m) alluvial-fan package of probable Holocene–upper Pleistocene boulder- to pebble-sized gravel and sand with a stage II to I calcic soil. This upper sediment package overlies an older, middle Pleistocene gravel and sand alluvial-fan sediment package with a greater than 3-ft-thick (1-m) stage IV calcrete horizon that probably marks a buried alluvial-fan surface. Vertical offset on the upper sediment package is about 5 ft (1.5 m). Displacement of the lower, stage IV calcrete horizon cannot be measured along most of the scarp without excavation because the horizon is not exposed in most of the gullies on the

downthrown fault block. At one locality, however, along the southern part of the 3.1-mi-long (5-km) scarp, the stage IV calcrete horizon is vertically displaced 13 ft (4 m). It is unknown if the entire length of this fault has had the same rupture history. The approximate average slip rate since middle Pleistocene is low at ≤0.03 mm/yr, although relatively young upper Pleistocene–Holocene deposits are faulted. The average recurrence interval for large surface ruptures since middle Pleistocene is about 80,000 to 160,000 yr. The East Sierra Diablo fault's closest distance to the Faskin Ranch reference point is 23 mi (37 km).

West Delaware Mountains Fault Zone

The West Delaware Mountains fault zone (fault 24, figs. 1 and 11) trends northwest at N25°–45°W, dips southwest, and separates the west flank of the Delaware Mountains from the deep part of the Salt Basin. This fault zone is about 40 mi (64 km) long and consists of multiple subparallel and en echelon fault strands. Most scarps are between 0.6 and 4.3 mi (1 and 7 km) long. At the northern part of the West Delaware Mountains fault zone, multiple northwest-striking faults form a broad, 1.8- to 3-mi-wide (3- to 5-km) zone. Aerial photograph investigation of the faults in this broad zone suggest that Quaternary geomorphic surfaces of different ages are offset different amounts, although our field studies only focused on one scarp that cuts two upper Pleistocene–Holocene(?) surfaces.

The scarp of the northwesternmost, 4.3-mi-long (7-km) fault strand of this zone has a slope as great as 11° and height up to 7.5 ft (2.3 m). Soils in this area are gypsiferous as well as calcic. Upper Pleistocene to Holocene(?) deposits having a soil with a stage II calcic morphology are displaced vertically about 5.2 ft (1.6 m). Where the scarp intersects a younger upper Pleistocene–Holocene(?) surface, the scarp is 4 ft (1.2 m) high and has a slope of 9°. Vertical displacement across the younger deposits that also have a stage II calcic soil morphology is 3 ft (0.9 m). Unfaulted arroyo terrace deposits are more than about 5,700 yr old, according to a corrected radiocarbon date of carbon (humic soil material) in the unfaulted terrace (R. Langford,

personal communication, 1993). The fault zone's closest distance to the Faskin Ranch reference point is 40 mi (64 km).

WILD HORSE FLAT BASIN FAULTS

East Carrizo Mountain–Baylor Mountain Fault

The 25.4-mi-long (41-km) Carrizo Mountain–Baylor Mountain fault (fault 7, figs. 1 and 11) separates the west side of Wild Horse Flat Basin from the Carrizo and Baylor Mountains. This fault strikes northeast at N10°–40°E and dips southeast. About 85 percent of this fault's length is covered and inferred. Three scarps along this fault are 0.6, 0.7, and 1.8 mi (1, 1.2, and 3 km) long. An eroded, subtle scarp located west-southwest of Van Horn has a scarp-slope angle of 5° and height of 6 ft (1.8 m). The faulted piedmont surface at this scarp has a stage IV calcrete, suggesting a middle Pleistocene age of the faulted surficial deposits. This horizon mostly is covered by a thin sequence of younger alluvium on the downthrown fault block. Locally on the upthrown fault block, Precambrian sandstone is at the surface. Vertical displacement of middle Pleistocene deposits is 5.2 ft (1.6 m). The average slip rate since the middle Pleistocene is ≤0.01 mm/yr. The average recurrence interval for large surface ruptures since the middle Pleistocene is approximately 125,000 to 250,000 yr. The East Carrizo Mountain–Baylor Mountain fault's closest distance to the Faskin Ranch reference point is 23 mi (37 km).

LOBO VALLEY BASIN FAULTS

The western edge of Lobo Valley Basin (figs. 1 and 11) is bounded by a 40.3-mi-long (65-km) fault zone that consists of four fault sections: (1) Fay fault (fault 13), (2) Neal fault (fault 16a), (3) Mayfield fault (fault 16b), and (4) Sierra Vieja fault (fault 16c). This range-bounding series of faults have very distinct scarps, and the zone is well expressed along most of its length. The West Lobo Valley fault zone has been called the Mayfield fault by Muehlberger

and others (1979, 1985) and Doser (1987). We use the name Mayfield (after Twiss, 1959) to refer to only one section of this long fault zone. The two southern sections of the zone, the Mayfield (fault 16b) and Sierra Vieja (fault 16c) faults, are the nearest Quaternary fault scarps to the approximate epicenter of the 1931 Valentine earthquake near Valentine, Texas (Doser, 1987; Davis and others, 1989). The northeast part of Lobo Valley is bounded by the West Wylie Mountains fault (fault 17). Another possible Quaternary fault, the Deep Well fault (fault 15), is located in the northern part of the Van Horn Mountains adjacent to Lobo Valley.

Fay Fault

The Fay fault (fault 13, figs. 1 and 11) is a short, 2.5-mi-long (4-km) fault located at the northern part of the Van Horn Mountains. This fault strikes north-northwest at N5°–20°W, dips east, and consists of two en echelon scarps. The scarp of the northern part of this fault has a scarp-slope angle of 13° and height of 4.6 ft (1.4 m). Surficial middle Pleistocene alluvial fan deposits with stage IV calcrete are vertically offset 4 ft (1.2 m). The average slip rate since the middle Pleistocene is ≤0.01 mm/yr. The average recurrence interval for large surface ruptures since the middle Pleistocene is about 125,000 to 250,000 yr. The Fay fault's closest distance to the Faskin Ranch reference point is 26.7 mi (43 km).

Neal Fault

The Neal fault (fault 16a, figs. 1 and 11), strikes northward at N10°W–N25°E, dips east, and is about 11 mi (18 km) long. This fault comprises a main 8.4-mi-long (13.6-m) scarp and several associated en echelon shorter scarps that are as much as 1.2 mi (2 km) long. One of the shorter scarps has a scarp-slope angle of 8° and height of 7 ft (2.2 m). Vertical offset of middle Pleistocene alluvial-fan gravel capped with a stage IV calcrete is 6 ft (1.8 m) across this short scarp, which is near the northern end of the Neal fault. The main 8.4-mi-long (13.6-km) scarp has a very distinct single slope, with slope angles ranging between 14° and 22° and heights

ranging between 5.2 and 15.7 ft (1.6 and 4.8 m). On the upthrown block, bedrock is shallow and locally is at the surface. Vertical offset of middle Pleistocene alluvial-fan deposits capped by a stage IV calcrete horizon is at least 16.4 ft (5 m). The stage IV calcrete horizon or multiple, less developed calcic horizons are presumed to be buried on the downthrown fault block. A possible upper Pleistocene–Holocene(?) alluvial surface with a stage II calcic soil is vertically offset at least 3 ft (1 m). The average slip rate since middle Pleistocene is approximately ≤0.05 mm/yr. The average recurrence interval for surface ruptures since the middle Pleistocene is approximately 60,000 to 125,000 yr. The Neal fault's closest distance to the Faskin Ranch reference point is 30 mi (48 km).

Mayfield Fault

The northwest-trending Mayfield fault (fault 16b, figs. 1 and 11) is about 12.4 mi (20 km) long. It strikes N30°–55°W and dips northeast. At one locality the fault dips 70° to 80°, and striations preserved along the fault surface indicate that slip has been normal, parallel to the fault's dip. It has a single-slope scarp with scarp-slope angles ranging between 18° and 23° and heights between 13 and 23 ft (4 and 7 m). Similar to the Neal scarp, bedrock is shallow and locally at the surface on the upthrown fault block. Vertical offset of middle Pleistocene alluvial-fan deposits capped by a stage IV calcrete is as much as 19.6 ft (6 m). Holocene(?) arroyo terrace deposits are not faulted.

At the gap between the southern Van Horn Mountains and northern Sierra Vieja, the Mayfield scarp is an obsequent fault scarp. At this locality, headward erosion of the southwest draining Van Horn Creek on the upthrown fault block has eroded away a relatively large volume of Cretaceous and Tertiary strata so that the head of Van Horn Creek valley lies at the fault. The valley on the upthrown block is about 100 ft (30 m) lower than the middle Pleistocene alluvial-fan surface on the downthrown block. The fan surface is capped by an approximately 3-ft-thick (1-m) stage IV to locally stage III calcic soil. The mountain

canyon/valley source area for the middle Pleistocene alluvial fan, which had built eastward into Lobo Valley, has been completely eroded away. Van Horn creek drains into the Rio Grande. We postulate that the combination of friable strata and base-level changes caused by Rio Grande incision and late Tertiary–Quaternary tectonism enabled the southwest draining Van Horn Creek to cut off and erode away the eastward-draining mountain source of the middle Pleistocene alluvial fan on the hanging-wall fault block.

A short, narrow, subsidiary graben that is about 1.2 mi (2 km) long and about 0.4 mi (0.6 km) wide lies east of the main range-bounding fault. Middle Pleistocene alluvial fan deposits are vertically displaced as much as 4 ft (1.2 m) across the small graben. The Mayfield fault's average slip rate since middle Pleistocene is ≤0.05 mm/yr. The average recurrence interval for large surface ruptures since the middle Pleistocene is approximately 50,000 to 100,000 yr. The Mayfield fault's closest distance to the Faskin Ranch reference point is 35.4 mi (57 km).

Sierra Vieja Fault

The Sierra Vieja fault (fault 16c, figs. 1 and 11) makes up the southern section of the fault series that bounds the western edge of Lobo Valley. The Sierra Vieja fault strikes northward at N30°W–N20°E, dips east, and is about 15.5 mi (25 km) long. It consists of multiple en echelon strands. Some of the strands have 15-ft-high (4.5-m) compound scarps with steep scarp-slope angles up to 20°. Similar to the Neal and Mayfield scarps, bedrock is shallow and locally is at the surface on the upthrown fault block. Vertical offset of possible middle Pleistocene alluvial-fan deposits is up to 27 ft (8.2 m) and offset of possible upper Pleistocene–Holocene(?) alluvial-fan deposits is up to 11.4 ft (3.5 m). The last surface rupture may have produced as much as 5 ft (1.5 m) of vertical displacement if the steep part of the compound scarp was caused by a single rupture. Holocene(?) arroyo terraces are not displaced by the fault. Landslide deposits, including boulder-sized material, exist along the flank of Sierra Vieja, although it is unknown if

the landslides were caused by seismic activity. The average slip rate since the middle Pleistocene is ≤0.1 mm/yr. The average recurrence interval for large surface ruptures since the middle Pleistocene is about 35,000 to 70,000 yr. The Sierra Vieja fault's closest distance to the Faskin Ranch reference point is 48 mi (77 km).

West Wylie Mountains Fault

The West Wylie Mountains fault (fault 17, figs. 1 and 11) separates the northern part of Lobo Valley from the Wylie Mountains and Canning Ridge. This fault is inferred to be about 12.4 mi (20 km) long. This fault was not studied on the ground, although aerial-photograph investigations indicate that two 0.6-mi-long (1-km) scarps having Tertiary–Quaternary basin-fill on the hangingwall block occur at the southwestern flank of the Wylie Mountains and west flank of Canning Ridge (south of Wylie Mountains). The scarp at the southwestern edge of the Wylie Mountains has Tertiary–Quaternary(?) alluvium faulted against Permian limestone. Quaternary(?) alluvial-fan deposits are faulted at the southern scarp west of Canning Ridge. The northern part of the fault has been mapped in Precambrian and Permian bedrock at two localities (Hay-Roe, 1957). The West Wylie Mountains fault strikes N10°–30°W and dips southwest. This fault's closest distance to the Faskin Ranch reference point is 30 mi (48 km).

Deep Well Fault

The 0.8-mi-long (1.3-km) Deep Well Fault (fault 15, figs. 1 and 11) is located at the northern part of the Van Horn Mountains. We do not know if this fault has ruptured during the Quaternary. Aerial photograph studies indicate that a sharp contact exists between Tertiary–Quaternary gravel deposits and Permian limestone along the fault's trace. The Deep Well fault strikes north-northwest at N10°–30°W and dips westward, and its closest distance to the Faskin Ranch reference point is 29 mi (47 km).

CONCLUSIONS

1. Fourteen Quaternary faults are within 31 mi (50 km) of the proposed Eagle Flat site (fig. 1 and table A-1). There are no Quaternary fault scarps in the Eagle Flat Basin, where the proposed repository site is located. The closest Quaternary fault scarp to the repository, West Eagle Mountains–Red Hills fault (fault 1, fig. 1), is located 8.4 mi (13.5 km) south of the proposed site in northern Red Light Bolson. The closest distance from the proposed repository to an inferred extension of this fault is 6.5 mi (10.5 km).

2. The West Eagle Mountains–Red Hills fault (fault 1, fig. 1 and tables A-1 and A-2), the closest Quaternary fault to the proposed repository, is inferred to be 24.8 mi (40 km) long, but only 12 mi (19.5 km) have a dissected surface expression. It strikes N25°–55°W and dips southwestward. Near the surface this fault dips between 85° and 88°. Studies of this fault's scarp and of a trench across this fault indicate there probably have been three surface ruptures since the middle Pleistocene. Throw for the surface-rupture events was between 1.6 and 4.3 ft (0.5 and 1.3 m). Throws of middle Pleistocene and middle-upper Pleistocene deposits, respectively, are 8.2 ft (2.7 m) and 1.6 ft (0.5 m). In the trench, fractures are not visible across the fault in the upper 8 to 12 inches (20 to 30 cm) of the calcic horizon at the surface. We postulate that postfaulting soil forming processes have obscured the upper part of the fault and that the last surface rupture was probably during latest middle Pleistocene or early late Pleistocene (fig. 3). The approximate average slip rate of the West Eagle Mountains–Red Hills fault since the middle Pleistocene is <0.02 mm/yr. The average recurrence interval for large surface ruptures since middle Pleistocene is about 80,000 to 160,000 yr.

3. Lengths of most Quaternary faults are between about 11 and 24.8 mi (18 and 40 km) (fig. 1 and table A-1). Many of the faults are sections of longer fault zones that are between 43 and 64 mi (70 and 105 km) long. Strikes of individual faults are variable, although most of the fault zones strike northwestward or northward (fig. 1 and table A-1). Faults dip between 60° and 88° near the surface. Available seismic reflection data in the Hueco Bolson indicate most of the

Quaternary faults dip between 50° and 80° in the subsurface. It is unknown whether the faults become listric at depths greater than 2 mi (3.5 km) because of the depth limit of seismic resolution (Collins and Raney, 1991c).

4. Average slip rates since middle Pleistocene are ≤0.25 mm/yr, and most of the Quaternary faults have average slip rates of ≤0.1 mm/yr (table A-2). The maximum amount of throw during single surface rupture events (table A-2) was between 1.6 and 10 ft (0.5 and 3 m). Cumulative throw of middle Pleistocene deposits (table A-2) across the Quaternary faults ranges between 3 and 105 m (1 and 32 m). At least eight faults (table A-2) vertically displace upper Pleistocene deposits about 3 to 20 ft (1 to 6 m). Aerial-photograph studies of faulted areas not investigated on the ground suggest that several other faults, including the Central Amargosa fault (fault 11b), Southeast Amargosa fault (fault 11c), North Sierra Diablo fault (fault 22), probably cut upper Pleistocene or younger deposits.

5. Precise ages of the latest surface ruptures of the Quaternary faults are unknown. There have been no historical surface ruptures in the region. Average recurrence intervals for large surface ruptures having approximately 3 to 6.5 ft (1 to 2 m) of throw are relatively long (table A-2). The average recurrence interval for large surface ruptures since the middle Pleistocene for the East Franklin Mountains fault (fault 28), one of the most active faults of the region, is estimated to be 15,000 to 30,000 yr. Average recurrence intervals since the middle Pleistocene for most of the faults are approximately 50,000 to 160,000 yr. Faults that have probably ruptured during the Holocene include the East Franklin Mountains fault (fault 28a) and some faults of the Amargosa fault zone (faults 11a, 11b and 11c). These faults have scarps in probable Holocene deposits and vertically displace upper Pleistocene deposits as much as 15 to 20 ft (4.5 to 6 m), suggesting multiple upper Pleistocene–Holocene ruptures. Other faults that cut upper Pleistocene deposits, including the West Indio Mountains fault (fault 3), East Flat Top Mountains fault (fault 21), East Sierra Diablo fault (fault 8), faults of the West Delaware Mountains fault zone (fault 24), Neal fault (fault 16a), Sierra Vieja fault (fault 16c), and probably

the North Sierra Diablo fault (fault 22), may have ruptured during the Holocene or late Pleistocene.

6. Some faults that have had multiple ruptures since the middle Pleistocene and that vertically displace middle Pleistocene deposits by relatively large amounts, 23 to 59 ft (7 to 18 m), do not intersect younger deposits where we studied them on the ground. These faults include the Northwest Campo Grande fault (fault 12a), Acala fault (fault 26), and Mayfield fault (fault 16b). Holocene movement on these faults cannot be verified or ruled out without more detailed studies. Multiple ruptures and relatively large throws on middle Pleistocene deposits are not firm evidence for upper Pleistocene–Holocene displacement as evidenced by detailed studies (Collins and Raney, 1990, 1991a, b, c) of the Southeast Campo Grande fault (fault 12c). The Southeast Campo Grande fault has had five episodes of movement since middle Pleistocene and vertically displaces middle Pleistocene deposits 33 ft (10 m); however, the fault does not cut upper Pleistocene deposits.

ACKNOWLEDGMENTS

This research was funded by the Texas Low-Level Radioactive Waste Disposal Authority under Interagency Contract No. IAC(92-93)-0910. Helpful comments on this work were made by P. W. Dickerson; however, the final responsibility for this report lies with the authors. Final word processing was by Susan Lloyd, drafting was by Susan Krepps, and report assembly was by Jamie H. Coggin.

REFERENCES

Akersten, W. A., 1967, Red Light local fauna (Blancan), southeastern Hudspeth County, Texas: The University of Texas at Austin, Master's thesis, 168 p.

Albritton, C. C., Jr., and Smith, J. F., Jr., 1965, Geology of the Sierra Blanca area, Hudspeth County Texas: U.S. Geological Survey Professional Paper 479, 131 p.

Aldrich, M. J., Jr., Chapin, C. E., and Laughlin, A. W., 1986, Stress history and tectonic development of the Rio Grande rift, New Mexico: Journal of Geophysical Research, v. 91, no. B6, p. 6199–6211.

Barnes, J. R., Shlemon, R. J., and Slemmons, D. B., 1989a, The Amargosa fault: a previously unstudied major active fault in northern Chihuahua, Mexico (abs.): Association of Engineering Geologists Abstracts and Program, 32nd Annual Meeting, p. 50–51.

Barnes, J. R., Peizhen, Zhang, and Slemmons, D. B., 1989b, The Campo Grande fault zone: a source for focused ground motion at the proposed low-level radioactive waste disposal site, Hudspeth County, Texas (abs.): Association of Engineering Geologists Abstracts and Program, 32nd Annual Meeting, p. 50.

Beehner, T. S., 1990, Burial of fault scarps along the Organ Mountains fault, South-Central New Mexico: Bulletin of the Association of Engineering Geologists, v. 27, no. 1, p. 1–9.

Belcher, R. C., Goetz, L. K., and Muehlberger, W. R., 1977, Map B—Fault scarps within Quaternary units in west Texas, *in* Goetz, L. K., 1977, Quaternary faulting in Salt Basin graben, West Texas: The University of Texas at Austin, Master's thesis, scale 1:500,000.

Bell, J. J., 1963, Geology of the foothills of Sierra de los Pinos, northern Chihuahua, near Indian Hot Springs, Hudspeth County, Texas: The University of Texas at Austin, Master's thesis, 83 p.

Braithwaite, P., 1958, Cretaceous stratigraphy of northern Rim Rock Country, Trans-Pecos Texas: University of Texas, Austin, Master's thesis, 95 p.

Bridges, L. W., 1959, Revised Cenozoic history of northern Rim Rock Country, Trans-Pecos Texas: University of Texas, Austin, Master's thesis, 74 p.

Bucknam, R. C., and Anderson, R. E., 1979, Estimation of fault-scarp ages from a scarp-height-slope-angle relationship: Geology, v. 7, no. 1, p. 11–14.

Byerly, Perry, 1934, The Texas earthquake of August 16, 1931: Bulletin of the Seismological Society of America, v. 24, p. 81–99 and 303–325.

Clutterbuck, D. B., 1958, Structure of northern Sierra Pilares, Chihuahua, Mexico: University of Texas, Austin, Master's thesis, 84 p.

Collins, E. W., and Raney, J. A., 1989, Quaternary history of the Campo Grande fault of the Hueco Basin, Hudspeth and El Paso Counties, Trans-Pecos Texas (abs.): Geological Society of America Abstracts with Programs, v. 21, no. 6, p. A202.

_____ 1990, Neotectonic history and structural style of the Campo Grande fault, Hueco Basin, Trans-Pecos Texas: The University of Texas at Austin, Bureau of Economic Geology Report of Investigations No. 196, 39 p., 3 pls.

_____ 1991a, Neotectonic history and geometric segmentation of the Campo Grande fault: A major structure bounding the Hueco basin, Trans-Pecos Texas: Geology, v. 19, no. 5, p. 493–496.

_____ 1991b, Quaternary faults near a proposed low-level radioactive waste repository in the Hueco Bolson of Trans-Pecos Texas: Bulletin of the West Texas Geological Society, v. 30, no. 6, p. 5–11.

_____ 1991c, Tertiary and Quaternary structure and Paleotectonics of the Hueco basin, Trans-Pecos Texas and Chihuahua, Mexico: The University of Texas at Austin, Bureau of Economic Geology Geological Circular 91-2, 44 p.

_____ 1992, Quaternary faults near the proposed Eagle Flat low-level radioactive waste repository, Trans-Pecos Texas (abs.): Geological Society of America Abstracts with Programs, v. 24, no. 7, p. A35.

_____ 1993, Quaternary faults of west Texas (abs.): Geological Society of America Abstracts with Programs, v. 25, no. 5, p. A22.

Coordinación General de los Servicios Nacionales de Estadística, 1982, San Antonio El Bravo: Carta Geologica, Dirección General de Geografia, scale 1:250,000.

Dasch, E. J., 1959, Dike swarm of northern Rim Rock Country: University of Texas, Austin, Master's thesis, 62 p.

Davis, S. D., Pennington, W. D., and Carlson, S. M., 1989, A compendium of earthquake activity in Texas: The University of Texas at Austin, Bureau of Economic Geology Geological Circular 89-3, 27 p., 4 microfiche in pocket.

DeFord, R. K., 1969, Some keys to the geology of northern Chihuahua, *in* Cordoba, D. A., Wengerd, S. A., and Shomaker, John, eds., Guidebook of the border region: New Mexico Geological Society, Twentieth Field Conference, p. 61–65.

DeFord, R. K., and Bridges, L. W., 1959, Tarantula Gravel, northern Rim Rock country, Trans-Pecos Texas: Texas Journal of Science, v. 11, p. 268–295.

DeFord, R. K., and Haenggi, W. T., 1971, Stratigraphic nomenclature of Cretaceous rocks in northeastern Chihuahua, *in* Seewald, Ken, and Sundeen, Dan, eds., The geologic framework of the Chihuahua Tectonic Belt: West Texas Geological Society Publication 71–59, p. 175–196.

Dickerson, E. J., 1966, Bolson fill, pediment, and terrace deposits of Hot Springs area, Presidio County, Trans-Pecos Texas: The University of Texas at Austin, Master's thesis, 100 p.

Dietrich, J. W., Owen, D. E., and Shelby, C. A., 1968, Van Horn–El Paso Sheet, Barnes, V. E., project director: The University of Texas at Austin, Bureau of Economic Geology Geologic Atlas of Texas, scale 1:250,000.

Doser, D. I., 1987, The 16 August 1931 Valentine, Texas, earthquake: evidence for normal faulting in west Texas: Bulletin of the Seismological Society of America, v. 77, p. 2005–2017.

_____ 1990, Seismological studies for the proposed low-level radioactive waste repository, Hudspeth County, Texas, *in* Keller, G. R., Doser, D. I., and Baker, Mark, Geophysical studies related to the proposed low-level radioactive waste repository, Hudspeth County, Texas: University of Texas at El Paso contract report IAC(90-91)0268 for the Texas Low-Level Radioactive Waste Disposal Authority, 27 p.

Dumas, D. B., 1980, Seismicity in the Basin and Range province of Texas and northeastern Chihuahua, Mexico, *in* Dickerson, P. W., Hoffer, J. M., and Callender, J. F., eds., Trans-Pecos region, southeastern New Mexico and West Texas: New Mexico Geological Society, 31st Annual Field Conference Guidebook, p. 77–81.

Dumas, D. B., Dorman, H. J., and Latham, G. V., 1980, A reevaluation of the August 16, 1931, Texas earthquake: Bulletin of the Seismological Society of America, v. 70, no. 4, p. 1171–1180.

Dyer, R., 1989, Structural geology of the Franklin Mountains, West Texas, *in* Muehlberger, W. R., and Dickerson, P. W., eds., Structure and stratigraphy of Trans-Pecos Texas: 28th International Geological Congress Field Trip Guidebook T317, p. 65–70.

Ferrell, A. D., 1958, Stratigraphy of northern Sierra Pilares, Chihuahua, Mexico: University of Texas, Austin, Master's thesis, 77 p.

Frantzen, D. R., 1958, Oligocene folding in Rim Rock Country, Trans-Pecos Texas: University of Texas, Austin, Master's thesis, 45 p.

Gates, J. S., White, D. E., Stanley, W. D., and Ackermann, H. D., 1980, Availability of fresh and slightly saline ground water in the basins of westernmost Texas: Texas Department of Water Resources Report 256, 108 p.

Gile, L. H., 1987, Late Holocene displacement along the Organ Mountains fault in southern New Mexico: New Mexico Bureau of Mines & Mineral Resources Circular 196, 43 p.

Gile, L. H., Peterson, F. F., and Grossman, R. B., 1966, Morphological and genetic sequences of carbonate accumulation in desert soils: Soil Science, v. 101, no. 5, p. 347–360.

Gile, L. H., Hawley, J. W., and Grossman, R. B., 1981, Soils and geomorphology in the Basin and Range area of southern New Mexico—guidebook to the Desert Project: New Mexico Bureau of Mines & Mineral Resources Memoir 39, 222 p.

Goetz, L. K., 1977, Quaternary faulting in Salt Basin graben, West Texas: The University of Texas at Austin, Master's thesis, 136 p.

_____ 1980, Quaternary faulting in Salt Basin graben, West Texas, *in* Dickerson, P. W., and Hoffer, J. M., eds., Trans-Pecos Region: New Mexico Geological Society, 31st Annual Field Conference, p. 83–92.

Gries, J. G., 1979, Problems of delineation of the Rio Grande Rift into the Chihuahua Tectonic Belt of northern Mexico, *in* Ricker, R. E., ed., Rio Grande rift: tectonics and magmatism: Washington, D.C., American Geophysical Union, p. 107–113.

_____1980, Laramide evaporite tectonics along the Texas–northern Chihuahua border, *in* Dickerson, P. W., and Hoffer, J. M., eds., Trans-Pecos region: New Mexico Geological Society, 31st Annual Field Conference, p. 93–100.

Gries, J. G., and Haenggi, W. T., 1971, Structural evolution of the eastern Chihuahua Tectonic Belt, *in* Seewald, Ken, and Sundeen, Dan, eds., The geologic framework of the Chihuahua Tectonic Belt: West Texas Geological Society, p. 119–138.

Groat, C. G., 1972, Presidio Bolson, Trans-Pecos Texas and adjacent Mexico: geology of a desert basin aquifer system: The University of Texas at Austin, Bureau of Economic Geology Report of Investigations No. 76, 46 p.

Gustavson, T. C., 1991, Arid basin depositional systems and paleosols: Fort Hancock and Camp Rice Formations (Pliocene–Pleistocene), Hueco Bolson, West Texas and adjacent Mexico: The University of Texas at Austin, Bureau of Economic Geology Report of Investigations No. 198, 49 p.

Hadi, Julfi, and Moss, Duncan, 1991, A study of the structure and geometry of the southeastern Hueco Bolson (abs.): Geological Society of America Abstracts with Programs, v. 23, no. 4, p. 28.

Haenggi, W. T., 1966, Geology of El Cuervo area, northeastern Chihuahua, Mexico: The University of Texas at Austin, Ph.D. dissertation, 402 p.

Harbour, R. L., 1972, Geology of the northern Franklin Mountains, Texas and New Mexico: U.S. Geological Survey Bulletin 1298, 129 p.

Harkey, D. A., 1985, Structural geology and sedimentologic analysis (Las Vigas Formation), Sierra San Ignacio, Chihuahua, Mexico: University of Texas at El Paso, Master's thesis, 122 p.

Hawley, J. W., 1975, Quaternary history of Dona Ana County region, south-central New Mexico, *in* Seager, W. R., Clemons, R. E., and Callender, J. F., eds., Las Cruces country: New Mexico Geological Society, 26th Annual Field Conference Guidebook, p. 139–140.

Hawley, J. W., Kottlowski, F. E., Seager, W. R., King, W. E., Strain, W. S., and LeMone, D. V., 1969, The Santa Fe Group in south-central New Mexico border region: New Mexico Bureau of Mines and Mineral Resources Circular 104, p. 52–76.

Hay-Roe, Hugh, 1957, Geology of Wylie Mountains and vicinity, Culberson and Jeff Davis Counties, Texas: The University of Texas at Austin, Bureau of Economic Geology Geologic Quadrangle Map No. 21, scale 1:63,360.

Henry, C. D., and Gluck, J. K., 1981, A preliminary assessment of the geologic setting, hydrology, and geochemistry of the Hueco Tanks geothermal area, Texas and New Mexico: The University of Texas at Austin, Bureau of Economic Geology Geological Circular 81-1, 47 p.

Henry, C. D., and McDowell, F. W., 1986, Geochronology of magmatism in the Tertiary volcanic field, Trans-Pecos Texas, *in* Price, J. G., Henry, C. D., Parker, D. F., and Barker, D. S., eds., Igneous geology of Trans-Pecos Texas, field trip guide and research articles: The University of Texas at Austin, Bureau of Economic Geology Guidebook 23, p. 99–122.

Henry, C. D., and Price, J. G., 1984, Variations in caldera development in the mid-Tertiary volcanic field of Trans-Pecos Texas: Journal of Geophysical Research, v. 89, no. B10, p. 8765–8786.

_____ 1985, Summary of the tectonic development of Trans-Pecos Texas: The University of Texas at Austin, Bureau of Economic Geology Miscellaneous Map No. 36, scale 1:500,000, 8 p.

_____ 1986, Early basin and Range development in Trans-Pecos Texas and adjacent Chihuahua: magmatism and orientation, timing, and style of extension: Journal of Geophysical Research, v. 91, no. B6, p. 6213–6224.

_____ 1989, Characterization of the Trans-Pecos Region, Texas: Geology, *in* Bedinger, M. S., Sargent, K. A., and Langer, W. H., eds., Studies of geology and hydrology in the Basin and Range Province, southwestern United States, for isolation of high-level radioactive waste—characterization of the Trans-Pecos Region, Texas: U.S. Geological Survey Professional Paper 1370-B, p. B4–B22.

Henry, C. D., Gluck, J. K., and Bockoven, N. T., 1985, Tectonic map of the Basin and Range province of Texas and adjacent Mexico: The University of Texas at Austin, Bureau of Economic Geology Miscellaneous Map No. 36, scale 1:500,000.

Henry, C. D., McDowell, F. W., Price, J. G., and Smyth, R. C., 1986, Compilation of potassium-argon ages of Tertiary igneous rocks, Trans-Pecos Texas: The University of Texas at Austin, Bureau of Economic Geology Geological Circular 86-2, 34 p.

Horak, R. L., 1985, Trans-Pecos tectonism and its effect on the Permian Basin, *in* Dickerson, P. W., and Muehlberger, W. R., eds., Structure and tectonics of Trans-Pecos Texas: West Texas Geological Society Field Conference, Publication No. 85-81, p. 81–87.

Izett, G. A., 1981, Volcanic ash beds: recorders of Upper Cenozoic silicic pyroclastic volcanism in the western United States: Journal of Geophysical Research, v. 86, no. B11, p. 10200–10222.

Izett, G. A., and Wilcox, R. E., 1982, Map showing localities and inferred distributions of the Huckleberry Ridge, Mesa Falls, and Lava Creek ash beds (Pearlette Family ash beds) of Pliocene and Pleistocene age in the western United States and Southern Canada: U.S. Geological Survey Miscellaneous Investigations Map I-1325, scale 1:4,000,000.

Jackson, M. L. W., Langford, R. P., and Whitelaw, M. J., 1993, Basin-fill stratigraphy, paleomagnetics and Quaternary history of the Eagle Flat study area, southern Hudspeth County, Texas: The University of Texas at Austin, Bureau of Economic Geology, contract report prepared for the Texas Low-Level Radioactive Waste Disposal Authority under interagency contract no. IAC(92-93)-0910, 53 p. plus appendices.

Jackson, M. L. W., and Whitelaw, M. J., 1992, Characteristics and paleomagnetic dating of thick buried vertisols, Trans-Pecos Texas (abs.): Geological Society of America Abstracts with Programs, v. 24, no. 7, p. A279.

Jones, B. R., and Reaser, D. F., 1970, Geology of southern Quitman Mountains, Hudspeth County, Texas: The University of Texas at Austin, Bureau of Economic Geology Geologic Quadrangle Map No. 39, scale 1:48,000, 24-p. text.

Keaton, J. R., 1993, Maps of potential earthquake hazards in the urban area of El Paso, Texas: Report for U.S. Geological Survey National Earthquake Hazards Reduction Program, Grant No. 1434-92-G-2171, 4 p.

Keaton, J. R., Shlemon, R. J., Slemmons, D. B., Barnes, J. R., and Clark, D. G., 1989, The Amargosa fault: a major late Quaternary intra-plate structure in northern Chihuahua, Mexico (abs.): Geological Society of America Abstracts with Programs, v. 21, no. 6, p. A148.

Keller, G. R., and Peeples, W. J., 1985, Regional gravity and aeromagnetic anomalies in west Texas, *in* Dickerson, P. W., and Muehlberger, W. R., eds., Structure and tectonics of Trans-Pecos Texas: West Texas Geological Society Publication 85-81, p. 101–105.

Kelson, K. I., Hemphill-Haley, M. A., Wong, I. G., Gardner, J. N., and Reneau, S. L., 1993, Paleoseismologic studies of the Pajarito fault system, western margin of the Rio Grande Rift near Los Alamos, New Mexico (abs.): Geological Society of America Abstracts with Programs, v. 25, no. 5, p. 61–62.

King, P. B., 1948, Geology of the southern Guadalupe Mountains, Texas: U.S. Geological Survey Professional Paper 215, 183 p.

_____ 1965, Geology of the Sierra Diablo region, Texas: U.S. Geological Survey Professional Paper 480, 185 p.

LeMone, D. V., 1984, Aspects of border region geology from the Tom Lea Park overlook, El Paso, Texas, *in* Clark, K. F., Gerald, R. E., Bridges, L. W., Dyer, R., and LeMone, D. V., leaders, Geology and petroleum potential of Chihuahua, Mexico: West Texas Geological Society Field Trip Guidebook, Publication No. 84-80, p. 104–111.

Langford, R. P., 1993, Landscape evolution in the Eagle Flat and Red Light basins, Chihuahuan Desert, south central Trans-Pecos Texas: The University of Texas at Austin, Bureau of Economic Geology, contract report prepared for the Texas Low-Level Radioactive Waste Disposal Authority under interagency contract no. IAC(92-93)-0910, 79 p. plus appendices.

Lovejoy, E. M. P., 1971, Tectonic implications of high level surfaces bordering Franklin Mountains, Texas: Geological Society of America Bulletin, v. 82, no. 2, p. 433–445.

_____ 1972, Basin Range faulting rates, Franklin Mountains, Texas (abs.): Geological Society of America Abstracts with Programs, v. 4, no. 6, p. 387–388.

_____ 1975, An interpretation of the structural geology of the Franklin Mountains, Texas, *in* Seager, W. R., Clemons, R. E., and Callender, J. F., eds., Las Cruces country: New Mexico Geological Society, 26th Annual Field Conference Guidebook, p. 261–268.

Lovejoy, E. M. P., and Hawley, J. W., 1978, El Paso to New Mexico–Texas State Line, *in* Hawley, J. W., ed., Guidebook to the Rio Grande rift in New Mexico and Colorado: New Mexico Bureau of Mines & Mineral Resources Circular 163, p. 57–68.

Machette, M. N., 1978a, Bernalillo County dump fault, *in* Hawley, J. W., ed., Guidebook to Rio Grande rift in New Mexico and Colorado: New Mexico Bureau of Mines & Mineral Resources Circular 163, p. 153–155.

_____ 1978b, Dating Quaternary faults in the southwestern United States by using buried calcic paleosols: U.S. Geological Survey, Journal of Research, v. 6, no. 3, p. 369–381.

_____ 1982, Quaternary and Pliocene faults in the La Jencia and southern part of the Albuquerque-Belen Basins, New Mexico: evidence of fault history from fault-scarp morphology and Quaternary geology, *in* Wells, S. G., Grambling, J. A., and Callender, J. F., eds., Albuquerque country II: New Mexico Geological Society, 33rd Annual Field Conference Guidebook, p. 161–169.

_____ 1985, Calcic soils of the southwestern United States, *in* Weide, D. L., ed., Soils and Quaternary geology of the southwestern United States: Geological Society of America Special Paper 203, p. 1–21.

_____ 1987, Preliminary assessment of paleoseismicity at White Sands Missile Range, southern New Mexico: evidence for recency of faulting, fault segmentation, and repeat intervals for major earthquakes in the region: U.S. Geological Survey Open-File Report 87-444, 46 p.

_____ 1988, Quaternary movement along the La Jencia fault, central New Mexico: U.S. Geological Survey Professional Paper 1440, 82 p.

Mack, G. H., and Seager, W. R., 1990, Tectonic control on facies distribution of the Camp Rice and Palomas Formations (Pliocene–Pleistocene) in the southern Rio Grande rift: Geological Society of America Bulletin, v. 102, no. 1, p. 45–53.

Mattick, R. E., 1967, A seismic and gravity profile across the Hueco Bolson, Texas: U.S. Geological Survey Professional Paper 575-D, p. 85–91.

McFadden, L. D., and Tinsley, J. C., 1985, Rate and depth of pedogenic-carbonate accumulation in soils: formulation and testing of a compartment model, *in* Weide, D. L., ed., Soils and Quaternary geology of the Southwestern United States: Geological Society of America Special Paper 203, p. 23–41.

Menges, C. M., 1987, Temporal and spatial segmentation of Pliocene–Quaternary fault rupture along the western Sangre de Cristo mountain front, northern New Mexico, *in* Crone, A. J., and Omdahl, E. M., eds., Directions in paleoseismology: U.S. Geological Survey Open-File Report 87-673, p. 202–222.

_____ 1990, Late Quaternary fault scarps, mountain-front landforms, and Pliocene–Quaternary segmentation on the range-bounding fault zone, Sangre de Cristo Mountains, New Mexico, *in* Krinitzsky, E. L., and Slemmons, D. B., Neotectonics in earthquake evaluation: Boulder, Colorado, Geological Society of America Reviews in Engineering Geology, v. 8, p. 131–156.

Milton, A. P., 1964, Geology of Cajoncito area in Municipio de Guadalupe, Chihuahua, and Hudspeth County, Texas: The University of Texas at Austin, Master's thesis, 78 p.

Morgan, Paul, Seager, W. R., and Golombek, M. P., 1986, Cenozoic thermal, mechanical and tectonic evolution of the Rio Grande rift: Journal of Geophysical Research, v. 91, no. B6, p. 6263–6276.

Morrison, R. B., 1969, Photointerpretive mapping from space photographs of Quaternary geomorphic features and soil associations in northern Chihuahua and adjoining New Mexico and Texas, *in* Cordoba, D. A., Wengerd, S. A., and Shomaker, John, eds., Guidebook of the border region, Chihuahua and the United States: New Mexico Geological Society, 20th Field Conference, p. 116–129.

Morrison, R. B., 1991, Introduction, *in* Morrison, R. B., ed., Quaternary nonglacial geology; conterminous U.S.: Geological Society of America, The Geology of North America, v. K-2, p. 1–14.

Muehlberger, W. R., 1980, Texas lineament revisited, *in* Dickerson, P. W., and Hoffer, J. M., eds., Trans-Pecos region, southwestern New Mexico and West Texas: New Mexico Geological Society, 31st Annual Field Conference Guidebook, p. 113–121.

Muehlberger, W. R., Belcher, R. C., and Goetz, L. K., 1978, Quaternary faulting in Trans-Pecos Texas: Geology, v. 6, no. 6, p. 337–340.

_____ 1985, Quaternary faulting in Trans-Pecos Texas, *in* Dickerson, P. W., and Muehlberger, W. R., eds., Structure and tectonics of Trans-Pecos Texas: West Texas Geological Society Publication 85-81, p. 21.

Muehlberger, W. R., and Dickerson, P. W., 1989, A tectonic history of Trans-Pecos Texas, *in* Muehlberger, W. R., and Dickerson, P. W., eds., Structure and stratigraphy of Trans-Pecos Texas: 28th International Geological Congress Field Trip Guidebook T317, p. 35–54.

Personius, S. F., and Machette, M. N., 1984, Quaternary and Pliocene faulting in the Taos Plateau region, Northern New Mexico, *in* Baldridge, W. S., Dickerson, P. W., Riecker, R. E., and Zidek, Jiri, eds., Rio Grande Rift: Northern New Mexico, New Mexico Geological Society, 35th Annual Field Conference Guidebook, p. 83–90.

Price, J. G., and Henry, C. D., 1984, Stress orientations during Oligocene volcanism in Trans-Pecos Texas: timing the transition from Laramide compression of Basin and Range tension: Geology, v. 12, no. 4, p. 238–241.

_____ 1985, Summary of Tertiary stress orientations and tectonic history of Trans-Pecos Texas, *in* Dickerson, P. W., and Muehlberger, W. R., eds., Structure and tectonics of Trans-Pecos Texas: West Texas Geological Society Publication No. 85-81, p. 149–151.

Ramberg, I. B., Cook, F. A., and Smithson, S. B., 1978, Structure of the Rio Grande rift in southern New Mexico and West Texas based on gravity interpretation: Geological Society of America Bulletin, v. 89, no. 1, p. 107–123.

Raney, J. A., and Collins, E. W., 1993, Regional geologic setting of Eagle Flat study area, Hudspeth County, Texas: The University of Texas at Austin, Bureau of Economic Geology, contract report prepared for the Texas Low-Level Radioactive Waste Disposal Authority under interagency contract no. IAC(92-93)-0910, 52 p.

Reagor, B. G., Stover, C. W., and Algermissen, S. T., 1982, Seismicity map of the state of Texas: Denver, Colorado, U.S. Geological Survey Miscellaneous Field Studies Map MF-1388, scale 1:1,000,000.

Richardson, G. B., 1909, Description of the El Paso district: U.S. Geological Survey, Geologic Atlas of the United States, El Paso Folio No. 166, scale 1:250,000.

Riley, R., 1984, Stratigraphic facies analysis of the upper Santa Fe Group, Fort Hancock and Camp Rice formations, far west Texas and south-central New Mexico: The University of Texas at El Paso, Master's thesis, 108 p.

Sanford, A. R., and Toppozada, T. R., 1974, Seismicity of proposed radioactive waste disposal site in southeastern New Mexico: New Mexico Bureau of Mines and Mineral Resources Circular 143, 15 p.

Sayre, A. N., and Livingston, Penn, 1945, Ground-water resources of the El Paso area, Texas: U.S. Geological Survey Water-Supply Paper 919, 190 p.

Seager, W. R., 1980, Quaternary fault system in the Tularosa and Hueco Basins, southern New Mexico and West Texas, *in* Dickerson, P. W., and Hoffer, J. M., eds., Trans-Pecos region, southwestern New Mexico and West Texas: New Mexico Geological Society, 31st Annual Field Conference, p. 131–135.

_____ 1981, Geology of Organ Mountains and southern San Andres Mountains, New Mexico: New Mexico Bureau of Mines & Mineral Resources Memoir 36, 98 p.

Seager, W. R., Shafiqullah, M., Hawley, J. W., and Marvin, R. F., 1984, New K-Ar dates from basalts and the evolution of the southern Rio Grande rift: Geological Society of America Bulletin, v. 95, no. 1, p. 87–99.

Seager, W. R., and Morgan, P., 1979, Rio Grande rift in southern New Mexico, West Texas, and northern Chihuahua, *in* Riecker, R. E., ed., Rio Grande rift: tectonics and magmatism: Washington, D.C., American Geophysical Union, p. 87–106.

Sellards, E. H., 1932, The Valentine, Texas, earthquake: The University of Texas Bulletin No. 3201, p. 113–138.

Sergent, Hauskins, and Beckwith, consulting geotechnical engineers, 1989, Preliminary geologic and hydrologic evaluation of the Fort Hancock site (NTP-S34), Hudspeth County, Texas, for the disposal of low-level radioactive waste: report prepared for Hudspeth County, Texas, Hudspeth County Conservation and Reclamation District No. 1, Hudspeth County Underground Water Conservation District No. 1, and El Paso County, Texas, SHB Job No. E88-4008B, p. 5-1–5-52.

Stevens, J. B., and Stevens, M. S., 1985, Basin and Range deformation and depositional timing, Trans-Pecos Texas, *in* Dickerson, P. W., and Muehlberger, W. R., eds., Structure and tectonics of Trans-Pecos Texas: West Texas Geological Society Field Conference, Publication 85-81, p. 157–163.

Strain, W. S., 1964, Blancan mammalian fauna and Pleistocene formations, Hudspeth County, Texas: University of Texas at Austin, Ph.D. dissertation, 148 p.

_____ 1966, Blancan mammalian fauna and Pleistocene formations, Hudspeth County, Texas: Texas Memorial Museum Bulletin No. 10, 55 p.

_____ 1971, Late Cenozoic bolson integration in the Chihuahua tectonic belt, *in* Hoffer, J. M., ed., Geologic framework of the Chihuahua tectonic belt, West Texas Geological Society Publication 71-59, p. 167–173.

Stuart, C. J., and Willingham, D. L., 1984, Late Tertiary and Quaternary fluvial deposits in the Mesilla and Hueco bolsons, El Paso area, Texas: Sedimentary Geology, v. 38, p. 1–20.

Thompson, J. S., 1991, Geology of the Washboard hills landslide, Hudspeth County, Texas (abs.): Geological Society of America, Abstracts with Programs, v. 23, no. 4, p. A98–99.

Twiss, P. C., 1959, Geology of Van Horn Mountains, Texas: The University of Texas at Austin, Bureau of Economic Geology Geologic Quadrangle Map No. 23, scale 1:48,000.

_____ 1979, Marfa sheet, Barnes, V. E., project director: The University of Texas at Austin, Bureau of Economic Geology Geologic Atlas of Texas, scale 1:250,000.

Underwood, J. R., 1963, Geology of Eagle Mountains and vicinity, Hudspeth County, Texas: The University of Texas at Austin, Bureau of Economic Geology Geologic Quadrangle Map No. 26, scale 1:48,000, 32-p. text.

Vanderhill, J. B., 1986, Lithostratigraphy, vertebrate paleontology, and magnetostratigraphy of Plio-Pleistocene sediments in the Mesilla Basin, New Mexico: The University of Texas at Austin, Ph.D. dissertation, 305 p.

Wallace, R. E., 1977, Profiles and ages of young fault scarps, north-central Nevada: Geological Society of America, v. 88, no. 9, p. 1267–1281.

Wen, Cheng-Lee, 1983, A study of bolson fill thickness in the southern Rio Grande Rift, Southern New Mexico, West Texas, and Northern Chihuahua: The University of Texas at El Paso, Master's thesis, 73 p.

Wilson, J. A., 1971, Vertebrate biostratigraphy of Trans-Pecos Texas and northern Mexico, *in* Seewald, Ken, and Sundeen, Dan, eds., Geologic framework of the Chihuahua tectonic belt: West Texas Geological Society Publication 71-59, p. 159–166.

Wood, J. W., 1968, Geology of the Apache Mountains, Trans-Pecos Texas: The University of Texas at Austin, Bureau of Economic Geology Geologic Quadrangle Map No. 35, scale 1:63,360, 32-p. text.

Woodward, L. A., Callender, J. F., Seager, W. R., Chapin, C. E., Gries, J. C., Shaffer, W. L., and Zilinski, R. E., 1978, Tectonic map of Rio Grande rift region in New Mexico, Chihuahua, and Texas, *in* Hawley, J. W., ed., Guidebook to Rio Grande rift in New Mexico and Colorado: New Mexico Bureau of Mines & Mineral Resources Circular 163, sheet 2, scale 1:1,000,000.

Zoback, M. L., and Zoback, M. D., 1980, State of stress in the conterminous United States: Journal of Geophysical Research, v. 85, no. B11, p. 6113–6156.

_____ 1989, Tectonic stress field of the continental United States, *in* Pakiser, L. C., and Mooney, W. D., eds., Geophysical framework of the continental United States: Boulder, Colorado, Geological Society of America Memoir 172, p. 523–539.

Table A-1. Geometric characteristics of faults that offset Quaternary deposits.

Basin	Fault and location number	Inferred maximum length (km)	Minimum mappable length (km)	Regional strike	Regional dip direction	Closest distance to Faskin Ranch reference point[1] (km)
Southeast Hueco Bolson	Campo Grande–Arroyo Diablo–Caballo fault zone[2] six geometric sections:					
	12a Northwest Campo Grande fault[2]	21[3]	9	N40°–70°W	SW	72
	12b Middle Campo Grande fault[2]	21[3]	12	N40°–70°W	SW	64
	12c Southeast Campo Grande fault[2]	34[3]	23.5	N40°–70°W	SW	42
	10 Arroyo Diablo fault[2]	25[3]	15	N30°–60°W	SW	39
	2a North Caballo fault[2]	22	2.5	N20°–40°W	SW	23
	2b South Caballo fault[4]	26	11	N20°–40°W	SW	24
	Amargosa fault zone[2] three geometric sections:					
	11a Northwest Amargosa fault[2]	21	21	N40°–50°W	NE	62
	11b Central Amargosa fault[2]	35.5	35.5	N40°–50°W	NE	43
	11c Southeast Amargosa fault[2]	10	10	N40°–50°W	NE	41
	14 Arroyo Macho fault[2]	1.5	1.5	N30°–40°E	SE	44
	26 Acala fault[2]	10	10	N40°–50°W	SW	68
	4 Ice Cream Cone fault[2]	9	9	N15°–60°W	SW	29
	27 Schroeder fault[4]	≥18.5	ND	N30°–50°W	NE	29.5
Northwest Hueco Bolson	28a East Franklin Mountains fault[2]	25	23	N10°W–N10°E	E	138
	28b Southeast Franklin Mountains fault[2]	25	25	N10°W–N10°E	E	138
Red Light Bolson	East Red Light Bolson fault zone[2] two geometric sections:					
	1 West Eagle Mountains–Red Hills fault[2]	40	19.5	N25°–55°W	SW	10.5
	3 West Indio Mountains fault[2]	50	24	N30°–45°W	SW	34.5
	5 Nick Draw fault[4]	2.5	2.5	N10°–15°E	W	29

Table A-1 (cont.)

Basin	Fault and location number	Inferred maximum length (km)	Minimum mappable length (km)	Regional strike	Regional dip direction	Closest distance to Faskin Ranch reference point[1] (km)
Southeast Eagle Flat Basin	6 East Eagle Mountains fault[2]	5	0.5	N10°–20°W	E	32
	9 West Van Horn Mountains fault[4]	27	7	N30°W–N15°E	W	38.5
Green River Basin	East Green River fault zone[4] two geometric sections:					
	19 China Canyon fault[4]	1.5	1	N10°–20°W	E	52
	20 Green River fault[4]	5.5	5.5	N15°–30°W	SW	52
	18 Indio fault[4]	20	20	N20°–45°W	SW	39
Salt Basin	West Salt Basin fault zone[2] four geometric sections:					
	29 Dell City fault[4]	19	19	N45°–65°W	NE	72
	21 East Flat Top Mountain fault[2]	23	17	N25°W–N5°E	E	53
	22 North Sierra Diablo fault[2]	13.5	4	N75°–85°W	N	54
	8 East Sierra Diablo fault[2]	37	34	N10°W–N20°E	E	37
Wild Horse Flat Basin	7 East Carrizo Mountain–Baylor Mountain fault[2]	41	17.5	N10°–40°E	SE	37
Lobo Valley Basin	West Lobo Valley fault zone[2] four geometric sections:					
	13 Fay fault[2]	4	3.5	N5°–20°W	E	43
	16a Neal fault[2]	18	18	N10°W–N25°E	E	48
	16b Mayfield fault[2]	20	20	N30°–55°W	NE	57
	16c Sierra Vieja fault[2]	25	25	N30°W–N20°E	E	77
Salt Basin	24 West Delaware Mountains fault zone[2]	29	26	N25°–45°W	SW	64
Lobo Valley Basin	17 West Wylie Mountains fault[2]	20	13	N10°–30°W	SW	48

Table A-1 (cont.)

Basin		Fault and location number	Inferred maximum length (km)	Minimum mappable length (km)	Regional strike	Regional dip direction	Closest distance to Faskin Ranch reference point[1] (km)
not in a basin	15	Deep Well fault[4]	1.3	1.3	N10°–30°W	W	47
Llanos de Chilicote	23	Sierra de la Lagrina fault[4]	41	ND	N5°–35°W	W	61
	25	Sierra Labra fault[4]	22	ND	N0°–30°W	W	65

[1]Faskin Ranch reference point = 105°15′, longitude: 31°07′30″
[2]Normal fault with Quaternary displacement and distinct scarp
[3]Maximum length based on interpretations of seismic data
[4]Fault with late Tertiary displacement, no Quaternary displacement, or Quaternary displacement uncertain
ND = Not Determined

Table A-2. Fault displacement characteristics of faults that offset Quaternary deposits.

Basin	Fault and location number	Throw (m)			Throw (m) for single surface-rupture events	Approximate average slip rate (mm/yr) since middle Pleistocene[4]	Approximate range of average recurrence interval (yr) for surface ruptures since middle Pleistocene[5]
		Middle Pleistocene deposits[1]	Middle to upper Pleistocene deposits[2]	Upper Pleistocene deposits[3]			
Southeast Hueco Bolson	Campo Grande–Arroyo Diablo–Caballo fault zone						
	six geometric sections:						
	12a Northwest Campo Grande fault	14	ND	ND	ND	≤0.1	35,000–70,000
	12b Middle Campo Grande fault	ND	ND	ND	ND	ND	ND
	12c Southeast Campo Grande fault	10	3	NF	1–2.2	≤0.1	50,000–100,000
	10 Arroyo Diablo fault	1.6–3	NF	NF	≥0.6	≤0.02	125,000–250,000
	2a North Caballo fault	24 (approx.)	7	NF	1.7	≤0.2	20,000–40,000
	2b South Caballo fault	NF	NF	NF	ND	NF	NF
	Amargosa fault zone						
	three geometric sections:						
	11a Northwest Amargosa fault	23.5	6.5	2.5–4.5	1.5–2.5	≤0.2	20,000–40,000
	11b Central Amargosa fault	ND	6	ND	ND	ND	>20,000
	11c Southeast Amargosa fault	ND	ND	ND	ND	ND	ND
	14 Arroyo Macho fault	2	ND	ND	ND	≤0.01	125,000–250,000
	26 Acala fault	18	ND	ND	ND	≤0.1	30,000–60,000
	4 Ice Cream Cone fault	ND	13.8	NF	ND	≤0.1	>15,000
	27 Schroeder fault	NF	NF	NF	ND	NF	NF
Northwest Hueco Bolson	28a East Franklin Mountains fault	≥25–32	≥8.5	≥4.5–6	1.7–3	≤0.25	15,000–30,000
	28b Southeast Franklin Mountains fault	ND	ND	ND	ND	ND	ND
Red Light Bolson	East Red Light Bolson fault zone						
	two geometric sections:						
	1 West Eagle Mountains–Red Hills fault	2.7	0.5	NF	0.5–1.3	≤0.02	80,000–160,000
	3 West Indio Mountains fault	9 (approx.)	2.2–≥2.5	0.9–2.5	0.9–2.5	≤0.1	40,000–80,000
	5 Nick Draw fault	NF	NF	NF	ND	NF	NF

Table A-2 (cont.)

Basin	Fault and location number	Throw (m)			Throw (m) for single surface-rupture events	Approximate average slip rate (mm/yr) since middle Pleistocene[4]	Approximate range of average recurrence interval (yr) for surface ruptures since middle Pleistocene[5]
		Middle Pleistocene deposits[1]	Middle to upper Pleistocene deposits[2]	Upper Pleistocene deposits[3]			
Southeast Eagle Flat Basin							
	6 East Eagle Mountains fault	ND	ND	ND	ND	ND	ND
	9 West Van Horn Mountains fault	NF	NF	NF	ND	ND	ND
Green River Basin	East Green River fault zone two geometric sections:						
	19 China Canyon fault	ND	ND	ND	ND	ND	ND
	20 Green River fault	ND	ND	ND	ND	ND	ND
	18 Indio fault	ND	ND	NF	ND	ND	ND
Salt Basin	West Salt Basin fault zone four geometric sections:						
	29 Dell City fault	ND	ND	ND	ND	ND	ND
	21 East Flat Top Mountain fault	ND	ND	1.2	ND	ND	ND
	22 North Sierra Diablo fault	ND	ND	ND	ND	ND	ND
	8 East Sierra Diablo fault	4	ND	1.5	1.5	≤0.03	80,000–160,000
Wild Horse Flat Basin	East Carrizo Mountain–Baylor Mountain fault	1.6	ND	ND	ND	≤0.01	125,000–250,000
Lobo Valley Basin	West Lobo Valley fault zone four geometric sections:						
	13 Fay fault	1.2	ND	ND	ND	≤0.01	125,000–250,000
	16a Neal fault	≥5	ND	≥1	ND	≤0.05	60,000–125,000
	16b Mayfield fault	7.5	ND	ND	ND	≤0.05	50,000–100,000
	16c Sierra Vieja fault	≥8.2–≥11	≥3.4	3.5	1.5–2.2	≤0.1	35,000–70,000
Salt Basin	24 West Delaware Mountains fault zone	ND	ND	1.5	ND	ND	ND
Lobo Valley Basin	17 West Wylie Mountains fault	ND	ND	ND	ND	ND	ND

Table A-2 (cont.)

Basin		Fault and location number	Throw (m) Middle Pleistocene deposits[1]	Throw (m) Middle to upper Pleistocene deposits[2]	Throw (m) Upper Pleistocene deposits[3]	Throw (m) for single surface-rupture events	Approximate average slip rate (mm/yr) since middle Pleistocene[4]	Approximate range of average recurrence interval (yr) for surface ruptures since middle Pleistocene[5]
not in a basin	15	Deep Well fault	ND	ND	ND	ND	ND	ND
Llanos de Chilicote	23	Sierra de la Lagrina fault	ND	ND	ND	ND	ND	ND
	25	Sierra Labra fault	ND	ND	ND	ND	ND	ND

[1]Includes deposits that have stage IV to V calcic soils
[2]Includes deposits that have stage III to IV calcic soils
[3]Includes deposits that have stage II calcic soils
[4]Based on throw of middle Pleistocene deposits and youngest middle Pleistocene time of about 130,000 B.P.; maximum average rate
[5]Based on estimated number of large, 1- to 2-m surface ruptures since middle Pleistocene; assumes faulted middle Pleistocene deposits are approximately 250,000 to 500,000 yr old.
ND = Not Determined
NF = Not Faulted